

Washington University in St. Louis

## Washington University Open Scholarship

---

All Theses and Dissertations (ETDs)

---

1-1-2010

### The Role of Flue-Gas Recycle in Submicrometer Particle Formation during Oxy-Combustion of American and Chinese Coals

Selegha Daukoru

*Washington University in St. Louis*

Follow this and additional works at: <https://openscholarship.wustl.edu/etd>

---

#### Recommended Citation

Daukoru, Selegha, "The Role of Flue-Gas Recycle in Submicrometer Particle Formation during Oxy-Combustion of American and Chinese Coals" (2010). *All Theses and Dissertations (ETDs)*. 502. <https://openscholarship.wustl.edu/etd/502>

This Thesis is brought to you for free and open access by Washington University Open Scholarship. It has been accepted for inclusion in All Theses and Dissertations (ETDs) by an authorized administrator of Washington University Open Scholarship. For more information, please contact [digital@wumail.wustl.edu](mailto:digital@wumail.wustl.edu).

WASHINGTON UNIVERSITY IN ST. LOUIS  
School of Engineering and Applied Science  
Department of Energy, Environmental & Chemical Engineering

Thesis Examination Committee:  
Pratim Biswas, Chair  
Richard Axelbaum  
Jay Turner

THE ROLE OF FLUE-GAS RECYCLE IN SUBMICROMETER PARTICLE  
FORMATION DURING OXY-COMBUSTION OF AMERICAN AND CHINESE  
COALS

by

Selegha Michael Daukoru

A thesis presented to the School of Engineering  
of Washington University in partial fulfillment of the  
requirements for the degree of

MASTER OF SCIENCE

August 2010  
Saint Louis, Missouri

## ABSTRACT OF THE THESIS

The Role of Flue-Gas Recycle in Submicrometer Particle Formation during  
Oxy-Combustion of American and Chinese Coals

by

Selegha Michael Daukoru

Master of Science in Energy, Environmental & Chemical Engineering

Washington University in St. Louis, 2010

Research Advisor: Professor Pratim Biswas

During oxy-coal combustion, recycled flue gas is used as a diluent to replace  $N_2$  in pulverized coal-fired boilers and to moderate boiler temperatures. However, the effects of this combustion modality on submicrometer particle formation have yet to be fully investigated with the control of laboratory-scale experiments. A drop-tube furnace setup was used to investigate the role of flue-gas recycle on submicrometer particle formation from two American and four Chinese coals of differing ASTM ranks. Flue-gas recycle was found to have limited effect on the submicrometer particle size distribution for Powder River Basin coal ( $\Delta d_{pg} \leq 4$  nm) compared to without flue-gas recycle, and previous results of submicrometer particle formation with once-through systems retain their validity. Correlations were obtained among the fixed carbon contents of the American and Chinese coals and characteristics of measured particle size distributions such as the geometric mean size and total number concentration.

# Acknowledgments

I am grateful for the mentorship and belief of my adviser, Prof. Pratim Biswas, without whom this work would have been impossible. I am forever in his debt for all I have learned about the conduct of engineering research. Whatever merit may be found in the following pages is due to the strength of his example. I also thank the members of my thesis committee, Professors Richard Axelbaum and Jay Turner, for insights that have enriched this work and for generously agreeing to administer my examination.

I gratefully acknowledge Washington University's Consortium for Clean Coal Utilization for funding this work and the James M. McKelvey Scholarship for partial funding of my graduate study. I thank my colleagues and associates of the Aerosol & Air-Quality Research Laboratory (AAQRL), past and present, who have made my experience rich and memorable, including Drs. Ying Li and Achariya Suriyawong and Mr. Ken Peebles. Special thanks go to Prof. Ruth Chen for her great kindness and Drs. Wei-Ning Wang and Sarah Torkamani for their helpful suggestions. Many thanks to Lei Zhang for supplying the Chinese coals and assisting in their preparation, and to Woo-Jin An for help with SEM imaging.

This thesis is dedicated to those whose friendships continue to buoy my work and my aspirations.

S. Michael Daukoru

*Washington University in St. Louis*

*August 2010*

# Contents

Acknowledgments.....	iii
List of Tables .....	vi
List of Figures.....	vii
Chapter 1 Introduction.....	1
1.1 Background.....	2
1.2 Coal Classification.....	4
1.3 Coal Devolatilization.....	8
1.4 Submicrometer Particle Formation Mechanisms.....	9
1.4.1 Metal Vaporization.....	10
1.4.2 Metal-Oxide Vaporization.....	12
1.4.3 Soot Formation.....	13
1.5 Objectives of This Study .....	14
Chapter 2 Experimental Methods .....	15
2.1 Coal Feed System .....	16
2.2 Drop-Tube Furnace.....	17
2.3 Particle Sampling and Collection .....	18
2.3.1 Cascade Impactor .....	18
2.3.2 Scanning Mobility Particle Sizer (SMPS).....	18
2.3.3 Submicrometer Particle Collection .....	19
2.4 Flue-Gas Sampling .....	19
2.4.1 CO <sub>2</sub> Monitor.....	19
2.5 Experiment Test Plan.....	20
Chapter 3 Effect of O <sub>2</sub> /Coal Ratio on Submicrometer Particle Formation during Oxy-Combustion.....	22
3.1 Effect of Flame Temperature.....	22
3.2 Effect of Gas Composition .....	26
3.2.1 Coal-O <sub>2</sub> -N <sub>2</sub> System .....	27
3.2.2 Coal-O <sub>2</sub> -CO <sub>2</sub> System.....	29
3.3 Heat & Mass Transport Considerations.....	29
3.4 Results and Discussion .....	30
Chapter 4 Role of Flue-Gas Recycle in Submicrometer Particle Formation during Oxy-Combustion.....	36
4.1 Effect of Flue-Gas Recycle on Gas Composition.....	37
4.1.1 System Mole Balances for CO <sub>2</sub> .....	37
4.2 Results and Discussion .....	40

Chapter 5 Effect of Coal Composition on Submicrometer Particle Formation during Oxy-Combustion.....	44
5.1 Coal Sample Selection.....	44
5.1.1 American Coals.....	45
5.1.2 Chinese Coals.....	46
5.2 Coal Sample Characterization.....	46
5.3 Results and Discussion.....	50
Chapter 6 Summary & Conclusions.....	61
Appendix A Drop-Tube Furnace Temperature Profiles.....	64
Appendix B Flow Parameter Calculations for Drop-Tube Furnace Setup.....	65
Appendix C System Mole Balances for CO <sub>2</sub> .....	67
References.....	73
Vita.....	79

# List of Tables

Table 1.1 ASTM Standard Classification of Coal by Rank (D388-05).....	5
Table 2.1 Proximate Analysis, Ultimate Analysis, and Mineral Analysis for Powder River Basin Coal .....	20
Table 2.2 Summary of Experiment Plan.....	21
Table 3.1 Estimates of Adiabatic Flame Temperature for Varied O <sub>2</sub> /Coal Ratios in Coal-O <sub>2</sub> /N <sub>2</sub> and Coal-O <sub>2</sub> /CO <sub>2</sub> Systems .....	23
Table 3.2 Equilibrium Constant Coefficients for Vaporization Reactions of Typical Metal Oxides in Coals .....	25
Table 3.3 Calculated Equilibrium Constants for Metal-Oxide Reduction during Varied O <sub>2</sub> /Coal Ratios in Coal-O <sub>2</sub> /N <sub>2</sub> and Coal-O <sub>2</sub> /CO <sub>2</sub> Systems .....	25
Table 3.4 Calculated Sub-Oxide and Metal Partial Pressures from Metal-Oxide Reduction during Varied O <sub>2</sub> /Coal Ratios in Coal-O <sub>2</sub> /N <sub>2</sub> and Coal-O <sub>2</sub> /CO <sub>2</sub> Systems.....	31
Table 3.5 Summary Statistics for Submicrometer Particle Size Distributions during Combustion of PRB Coal with Varied O <sub>2</sub> /Coal Ratios.....	33
Table 4.1 Summary Statistics for Submicrometer Particle Size Distributions during Combustion of PRB Coal with Varied Flue-Gas Recycle Ratios at 1200 °C Furnace Temperature.....	41
Table 5.1 Mineral Fractions in Ash Content of Powder River Basin (PRB) and Illinois #6 Coal Samples.....	45
Table 5.2 Proximate and Ultimate Analyses for American & Chinese Coals.....	46
Table 5.3 Summary Statistics for Submicrometer Particle Size Distributions during Combustion of American & Chinese Coals during Conventional-Air and Oxy-Combustion Conditions.....	53

# List of Figures

Figure 1.1	Ash particle formation pathways during coal combustion .....	7
Figure 2.1	Drop-Tube Furnace Setup for Oxy-Combustion Experiments .....	16
Figure 3.1	Submicrometer Particle Size Distributions during Combustion of PRB Coal Varied O <sub>2</sub> /Coal Ratios in O <sub>2</sub> -N <sub>2</sub> Mixtures.....	32
Figure 3.2	Submicrometer Particle Size Distributions during Combustion of PRB Coal with Varied O <sub>2</sub> /Coal Ratios in O <sub>2</sub> -CO <sub>2</sub> Mixtures.....	33
Figure 3.3	Scatter Plot of Total Volume Concentration of Submicrometer Particles Sampled vs. Calculated Total Sub-Oxide Partial Pressures during Oxy-Coal Combustion at Varied O <sub>2</sub> /Coal Ratios.....	33
Figure 4.1	Drop-Tube Furnace Setup with Gas Mixture States during Steady Oxy-Combustion Operation.....	38
Figure 4.2	CO <sub>2</sub> Concentrations at Furnace Inlet and Adiabatic Flame Temperatures as a Function of Flue-Gas Recycle Ratio.....	39
Figure 4.3	Submicrometer Particle Size Distributions for Conventional Coal-Air Combustion and Oxy-Combustion at Varied Flue-Gas Recycle Ratios for PRB Coal .....	40
Figure 4.4	X-Ray Diffractograms of Submicrometer Particles Collected during Combustion of PRB Coal at Three Different Conditions .....	42
Figure 5.1	X-Ray Diffraction Spectra for Selected American & Chinese Coals .....	49
Figure 5.2	Submicrometer Particle Size Distributions for Conventional Coal-Air Combustion with American & Chinese Coals at a Fixed O <sub>2</sub> /Coal Molar Ratios .....	50
Figure 5.3	Submicrometer Particle Size Distributions for Oxy-Coal Combustion with American Coals at a Fixed Flue-Gas Recycle Ratio (40%).....	51
Figure 5.4	Submicrometer Particle Size Distributions for Oxy-Coal Combustion with Chinese Coals at a Fixed Flue-Gas Recycle Ratio (40%) .....	52
Figure 5.5	X-Ray Diffractogram of Submicrometer Particles Collected during Combustion of Illinois #6 Coal in Air .....	54
Figure 5.6	Scanning Electron Micrograph of Total Ash Particles Collected during Oxy-Combustion of S07 Coal.....	55
Figure 5.7	Scatter Plot of Total Number Concentration vs. Fixed Carbon Content for Submicrometer Particles Sampled during Coal-Air Combustion.....	55

Figure 5.8	Scatter Plot of Geometric Mean Diameter vs. Fixed Carbon Content for Submicrometer Particles Sampled during Coal-Air Combustion.....	56
Figure 5.9	Scatter Plot of Total Number Concentration vs. Fixed Carbon Content for Submicrometer Particles Sampled during Oxy-Coal Combustion with 40% Flue-Gas Recycle Ratio.....	57
Figure 5.10	Scatter Plot of Geometric Mean Diameter vs. Fixed Carbon Content for Submicrometer Particles Sampled during Oxy-Coal Combustion with 40% Flue-Gas Recycle Ratio.....	58

# Chapter 1

## Introduction

The relationships among energy resource extraction, energy conversion, energy use, human health, and the environment are complex, dynamic, and are of persisting importance for the following reasons: (1) Global demand for energy is projected to rise through 2030, driven by developing countries and principally China; (2) fossil fuels have been and are projected to be the predominant energy resources for decades to come, with coal consumption alone projected to average 1.7% growth annually from 2006 to 2030; and (3) fossil fuel extraction, conversion, and use are associated with negative environmental impacts.<sup>1,2</sup>

Oxy-combustion is one modality being developed for the capture and storage of CO<sub>2</sub> generated from the combustion of fossil fuels, primarily coal, and the goal of this thesis is to introduce and discuss implications of this mode of combustion on submicrometer particle formation, since submicrometer particles are known to be enriched in toxic trace metals<sup>3</sup>, preferentially penetrate air-pollution control devices (APCDs)<sup>4-8</sup>, harm human health and the environment when released into the atmosphere<sup>9-13</sup>, and have possibly negative impacts (such as fouling) on the CO<sub>2</sub> capture and storage processes which oxy-combustion is devised to facilitate<sup>14</sup>. It is therefore necessary to understand the formation mechanisms of submicrometer

particles under various combustion modalities, including oxy-coal combustion with flue gas recycle, and to do so at the laboratory scale where process parameters directly related to combustion can be more readily controlled.

## **1.1 Background**

Coal, primarily via pulverized coal (PC) combustion systems, accounts for 41% of global electricity generation, as much as 49% of electricity generation in the United States, and 81% in Mainland China. Coal combustion is the largest single contributor to global anthropogenic CO<sub>2</sub> emissions, contributing 42% of total CO<sub>2</sub> emissions<sup>15</sup> and 73% of the CO<sub>2</sub> emissions associated with electricity and heat use<sup>16</sup>. Similarly, in the United States, coal combustion contributes 81% of the CO<sub>2</sub> emissions from energy consumption in the electric utility sector<sup>17</sup>. Clearly, pulverized coal combustion is a major source of CO<sub>2</sub> emissions, and CO<sub>2</sub> emissions have well-documented effects on the global climate and the earth's energy balance<sup>2</sup>.

Oxy-coal combustion is one of several schemes devised for the control and capture of CO<sub>2</sub>. It features the replacement of air with O<sub>2</sub> while using recycled flue gas (RFG) as a diluent in the combustion mixture—the main advantage of which is the output of relatively high-purity CO<sub>2</sub> for geological sequestration, enhanced oil recovery, or other uses<sup>18-20</sup>. Such a concept for boiler design has ancillary advantages of reduced NO<sub>x</sub> emissions<sup>21-23</sup>, reduced flue gas volume<sup>19, 24</sup>, and heat

transfer characteristics replicating those of existing, conventional pulverized-coal boilers<sup>25</sup>. This combustion modality has the potential to be cheaper than post-combustion capture techniques such as CO<sub>2</sub> stripping using amines<sup>26, 27</sup>. However, the relationships between oxy-coal boiler design and emissions (gaseous and particulate) have required detailed study due to the observed and potential impacts of such emissions on human health and the environment<sup>9-13</sup>. Criteria for matching or improving combustion characteristics of new and retrofitted boilers compared to existing boilers, including criteria for scale-up, have also been required<sup>25</sup>.

As such, several laboratory-scale studies have considered various aspects of oxy-coal combustion, including ignition characteristics and flame propagation, char combustion, ash vaporization and particle formation, NO<sub>x</sub> reduction and SO<sub>x</sub> formation. Pilot-scale studies have also documented the feasibility of oxy-coal combustion at-scale and scale-up requirements; operational issues such as flame stability, char burnout, and gaseous pollutant emissions; and the optimization of oxy-coal combustion conditions to replicate radiative and convective heat transfer characteristics of conventional air-fired operation. These studies were well documented in the review by Buhre *et al.*<sup>19</sup> The feasibility of oxy-coal combustion is also being demonstrated on a pre-commercial pilot scale by a consortium led by the Swedish utility company, Vattenfall, which began operations at the 30-MW facility in at Schwarze Pumpe, Germany, in 2008<sup>28</sup>. Babcock and Wilcox has also demonstrated oxy-coal feasibility at the 30-MW scale since 2007, including new

burner design, flame stability, and operational issues involved in smoothly transitioning from air-fired to oxy-fired and vice-versa<sup>29</sup>. However, while many of the foregoing studies have investigated the effects of recycled flue gas on boiler performance, combustion efficiency, and gaseous pollutant emissions, only a few have studied submicrometer particle formation and toxic metal emissions,<sup>30-34</sup> and none have done so at the laboratory scale with actual (rather than simulated) recycled flue gas and with a variety of coal ranks. Thus, the objective of this thesis is to determine the role of flue-gas recycle in submicrometer particle formation during oxy-coal combustion of U.S. and Chinese coals.

## **1.2 Coal Classification**

Coal is a heterogeneous sedimentary rock resulting from the action of complex geochemical processes on plant precursors over time. Coal is also generally understood to be a carbonaceous material with mineral inclusions and inorganic associations within its porous structure. And, much effort has been expended to systematically classify coals and explain their geographical diversity by probing for the presence and extent of macromolecular networks that may constitute basic units of the chemical structure of coal. However, these efforts have had limited success due to lack of consensus in the literature as to the exact nature of the bonding between coal's constituent atoms and disputes over the applicability of molecular models purported to represent the structure of certain coal types.<sup>35</sup>

In spite of these difficulties, the American Society for Testing and Materials has promulgated a commonly used classification of coals by rank (ASTM D388-05). The ASTM classification has become a substitute for more detailed, but limited, characterization of coal samples and a useful tool for the valuation of coals, because there are well-known mappings between many physical and chemical properties of particular coals and their corresponding ASTM ranks<sup>36</sup>. The ASTM rank is specified by the fixed-carbon content of a coal and its calorific value, and it broadly classifies coals based on their degree of geologic aging (or coalification) into the following main classes, in order of decreasing age: (1) anthracite, (2) bituminous, (3) subbituminous, and (4) lignite. Each class is further divided into several groups, according to fixed-carbon content or calorific value, as detailed in Table 1.1.

**Table 1.1 ASTM Standard Classification of Coal by Rank (D388-05)<sup>35</sup>**

Class	Group	Fixed Carbon (%)	Calorific Value (Btu/lb)
(1) Anthracite	Meta-anthracite	≥ 98	-
	Anthracite	92-98	-
	Semianthracite	86-92	-
(2) Bituminous	Low-volatile bituminous	78-86	-
	Medium-volatile bituminous	69-78	-
	High-volatile A bituminous	< 69	≥ 14,000
	High-volatile B bituminous	< 69	13,000 - 14,000
	High-volatile C bituminous	< 69	11,500 - 13,000
(3) Subbituminous	Subbituminous A	< 69	10,500 – 11,500
	Subbituminous B	< 69	9,500 – 10,500
	Subbituminous C	< 69	8,300 – 9,500
(4) Lignite	Lignite A	< 69	6,300 – 8,300
	Lignite B	< 69	< 6,300

Two additional protocols are also used to characterize coal samples: (1) proximate analysis and (2) ultimate analysis. The proximate analysis characterizes coals based on the quantities of four constituents: char, volatile matter, moisture, and minerals. The ultimate analysis delineates the elemental composition of the combustible constituents of coal (i.e., the dry- and mineral-free coal). The amounts of char and volatile matter largely determine the calorific value of a given coal and therefore its burning behavior, while the mineral content originally included in the coal structure is the source of ash particles that are collected after char burning is complete (i.e. burnout). Figure 1.1 is a schematic of the coal burning process and main particle formation pathways, as described by Suriyawong *et al.*<sup>30</sup> The coal burning process and resulting particle formation pathways are briefly described as follows.

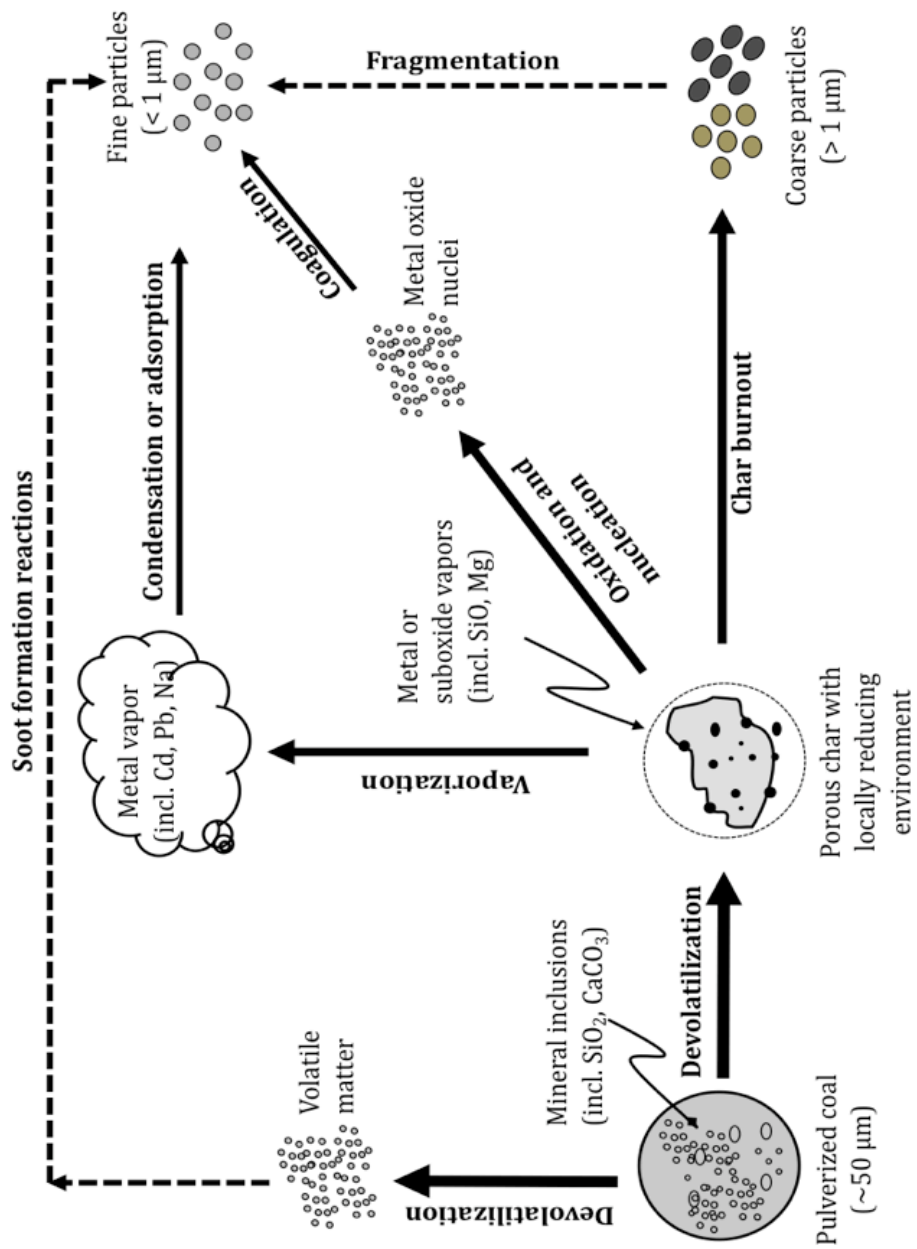


Figure 1.1 Ash particle formation pathways during coal combustion. Adapted from Suriyawong, *et al.*<sup>30</sup>

## 1.3 Coal Devolatilization

When a coal particle enters a high-temperature furnace or boiler environment, it undergoes distinct processes, some of which occur in sequence and some of which can occur simultaneously. The first of these processes is known as coal devolatilization, and it involves the thermally activated breakdown of weak C- bonds in the coal structure and the release of light, volatile hydrocarbon species. These volatile species, collectively referred to as volatile matter (VM) in proximate analyses of coal, diffuse away from the coal particle and undergo gas-phase reactions that evolve heat in the vicinity of the coal particle and advance the process of coal burning. Secondary reactions involving volatile matter can also produce tar and soot. The remaining material, which continues to undergo reaction with surrounding gases, is commonly known as char (or coal char). It is typically more enriched in carbon and still includes mineral compounds within its porous structure<sup>35</sup>.

Due to the complex and heterogeneous nature of coal particle structure and composition, the devolatilization process can include qualitatively unique phenomena. For instance, it has been widely observed that, in addition to the foregoing evolution of volatile material, bituminous coals tend to deform plastically during the devolatilization process, collapsing much of the porous structure of its char and impeding the outward pore diffusion of gases. Consequently, gas pockets or bubbles form, coalesce, and grow as they migrate to the char surface where they

then explode and induce fragmentation of the molten char and its mineral and metal-oxide inclusions. This breakup process has been used to explain some of the observed features of submicrometer particles, such as the presence of cenospheres and metal-oxide particles with collapsed structures, and a fragmentation pathway is included in Figure 1.1 to represent this possibility.

## **1.4 Submicrometer Particle Formation Mechanisms**

Using the same drop-tube furnace setup as used in this study, but in a once-through configuration, Suriyawong *et al.*<sup>30</sup> studied submicrometer particle formation mechanisms and mercury speciation during oxy-coal combustion and outlined possible routes along which trace metals partition into vapor or onto submicrometer and supermicrometer particles. Since temperature is one of the key parameters affecting the fate of trace metals during combustion, via its effect on the vaporization rates for volatile, toxic metals such as Hg, Suriyawong *et al.* also compared Hg speciation during conventional coal combustion (with air) with Hg speciation during oxy-coal combustion conditions. However, that laboratory-scale study did not include flue gas recycling, which is a key feature in full-scale oxy-coal combustion systems. According to Figure 1.1, which includes the major pathways for particle formation reported in the literature, the following processes related to submicrometer particle formation are described as follows.

### **1.4.1 Metal Vaporization**

Metal species are present in coal predominantly in the form of mineral oxides. However, trace amounts of metal exist in other forms throughout the coal structure and many exhibit relatively high volatility compared to the mineral metal oxides. The vaporization of these volatile metal species from coal has been extensively studied due to interest in their speciation and fate as well as due to interest in the capture of toxic metals liberated during coal combustion<sup>37-40</sup>. The vaporization of metal species and their role in submicrometer particle formation, while shown in Figure 1.1 to consist largely of a vaporization-nucleation-condensation pathway, has also been demonstrated to depend on many factors other than strictly the vapor pressure of particular metal species and thermodynamic equilibrium considerations. As discussed in the review by Linak<sup>37</sup>, factors such as the speciation of the metals within coal, proximity to other inorganic minerals, and the particular burning behavior of a coal type all complicate the release of metal species from the burning char. And, while toxic metal enrichment of submicrometer particles is of significant importance, more extensive characterization of the trace metals speciation in coal, coal mineral content, and the speciation of metals in ash would be required to explain the effect of flue-gas recycle on the submicrometer particles which may result from metal vaporization.

Understanding metal vaporization during coal combustion therefore requires a detailed knowledge of the speciation and partitioning of metals in coal as well as information about the interactions among metal species and other inorganic compounds in coal prior to consideration of the particular pathways through which these species appear as submicrometer particles. Yan *et al.*<sup>41</sup> addressed this task by modeling the partitioning of 16 trace metals under various coal combustion conditions, including varied temperatures (300-1800 K), varied reactant conditions (oxidizing and reducing), and different coal types. In all, 54 elements and 3200 compounds were accounted for in the modeling effort, resulting in 45 different species comprised of interactions between the 16 trace metals and other elements.

In spite of the demands in accounting for metal vaporization during coal combustion, a few researchers have performed more controlled experiments to clarify the particle formation mechanisms involving trace metal species. Mulholland and Sarofim<sup>42</sup> studied the fate of aqueous lead, cadmium and nickel nitrates fed through a laboratory-scale furnace. They observed that, in the case of nickel, which was not expected to follow a vaporization pathway for particle formation, submicrometer particles accounted for 30-35% of the total Ni particle mass. They hypothesized that bubble formation bursting in the nickel melt during the decomposition of nickel nitrate into nickel oxide and the evolution of nitrogen dioxide and oxygen were responsible for the submicrometer particles and micrometer-sized cenospheres observed. The formation of submicrometer particles of volatile trace metal species

via vaporization, nucleation, and condensation can therefore be supplemented by a pathway consisting of chemical transformation, bubble formation and bursting. However, species subject to this pathway tend to be present only in trace amounts relative to the total mineral content in coal.

### **1.4.2 Metal-Oxide Vaporization**

The formation of submicrometer particles during coal combustion has been well described mechanistically by several groups<sup>43-47</sup> and Figure 1.1 is a depiction of the main formation pathways described in the literature. Several studies have established that chemical nucleation from supersaturated metals or sub-oxides and growth by condensation and coagulation is the pathway that accounts for most of the submicrometer particle mass<sup>43-45</sup>. The reduction of metal-oxides by CO into more volatile metals and sub-oxides was assumed to be at equilibrium at the surface of burning char particles, as done by Suriyawong *et al.*<sup>30, 48</sup>. The partial pressure of metal or sub-oxide vapors thereby produced is a function of bulk O<sub>2</sub>-CO<sub>2</sub> concentrations as well as the temperature-dependent equilibrium constants for corresponding metal-oxides. Therefore, the bulk gas composition has direct and indirect effects on the vapor equilibria of volatile metals and sub-oxides generated by metal-oxide reduction—directly via the partial pressures of bulk O<sub>2</sub> and CO<sub>2</sub> and indirectly via their effect on the adiabatic flame temperature and the temperature-dependent equilibrium constants for metal-oxide reduction.

### 1.4.3 Soot Formation

During coal devolatilization, when volatile matter is being released from coal, secondary reactions can occur to form soot, which are the carbonaceous particle products of competing polymerization and cracking reactions that take place during devolatilization. Fletcher *et al.*<sup>49</sup> reviewed experiments related to soot formation in coal combustion systems and found that the primary particle size of coal-derived soot has been reported to be 25-60 nm, present in soot agglomerates up to 38  $\mu\text{m}$  in size. However, soot yields were only reported for coal pyrolysis experiments rather than in actual combustors, even though the soot formation process clearly depends on the gas composition and local gas and particle temperatures. It was also reported that soot formation largely depends on coal rank and coal particle size, with large ( $> 80 \mu\text{m}$ ), bituminous coal particles demonstrating the highest tendency to produce soot particles that emerge as tails on jets of volatile matter being released from the coal particle<sup>49</sup>. However, such soot particles were not observed from combustion of anthracite, small bituminous, and lignite particles.

More recent work by Veranth *et al.*<sup>50</sup> also reported observing a bimodal distribution of soot particles and aggregates produced during PC combustion of bituminous coal with a low-NO<sub>x</sub> pilot-scale burner. One mode consisted of soot aggregates associated with char particles  $> 10 \mu\text{m}$ , while the second mode consisted of dispersed soot particles in the submicrometer size range.

## 1.5 Objectives of This Study

Studies of particle formation during oxy-combustion performed so far have not involved flue-gas recycle, which is expected to affect bulk gas compositions in the combustion environment. Since bulk gas compositions have been found to affect submicrometer particle formation, the goal of this work was to investigate of the role of flue-gas recycle in submicrometer particle formation during oxy-coal combustion, and this was addressed in the following three parts:

- (1) Determining the effect of the O<sub>2</sub>/coal ratio on submicrometer particle formation in O<sub>2</sub>-N<sub>2</sub> systems and in O<sub>2</sub>-CO<sub>2</sub> systems.
- (2) Determining the effect of the flue-gas recycle ratio on submicrometer particle formation during oxy- (O<sub>2</sub>-CO<sub>2</sub>) combustion.
- (3) Determining the effect of coal composition (using American and Chinese coals) during conventional (coal-air) combustion and during oxy-combustion.

# Chapter 2

## Experimental Methods

The key components of the experimental setup, including a coal feed system, a drop-tube furnace, and sampling components for particles and flue gas, are depicted in Figure 2.1. This drop-tube furnace setup was modified to include the flue-gas recycling line from earlier configurations used by Smallwood<sup>51</sup> and Suriyawong<sup>52</sup>. These main system components, analytical methods used, the test plan and objectives for this work are briefly described as follows.

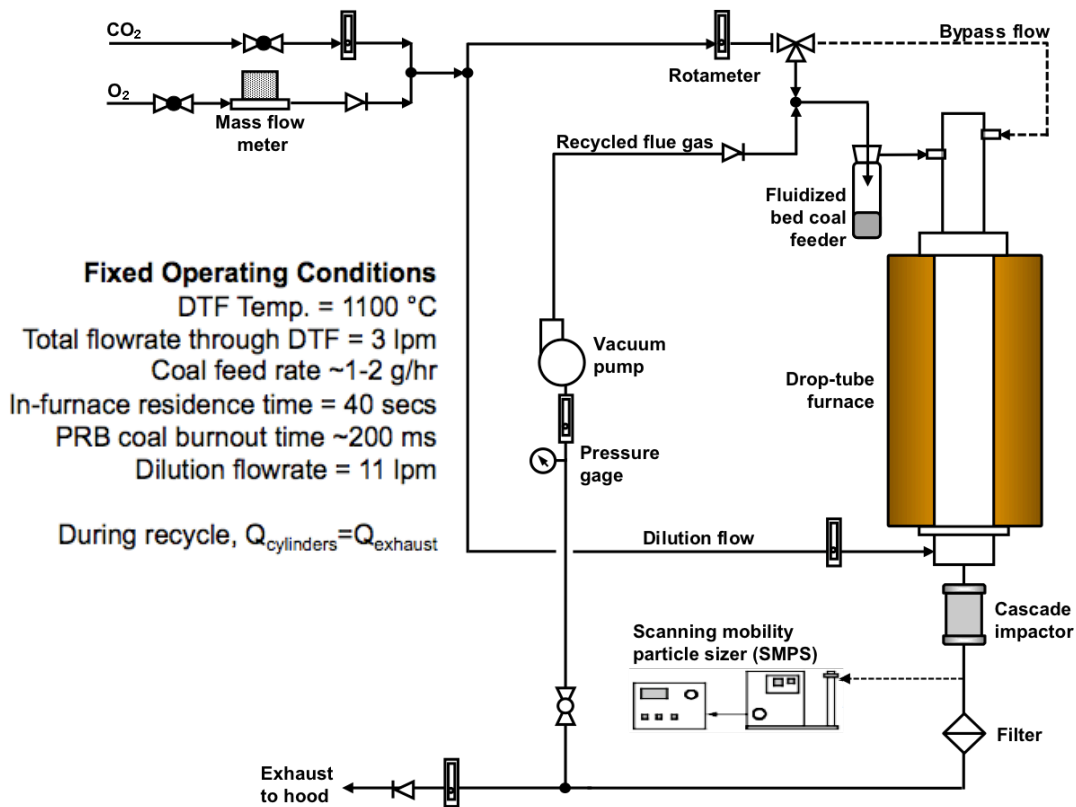


Figure 2.1 Drop-Tube Furnace Setup for Oxy-Combustion Experiments

## 2.1 Coal Feed System

Pulverized coal is fed into the furnace using a fluidized-bed coal feeder, consisting of a high velocity impinger (ACE Glass 7541-10) set, which is used to elutriate coal particles to be delivered into the furnace. Stokes' law can be used to estimate the maximum size of coal particles,  $d_{\text{max}}$ , that can be carried out of the impinger bottle (4-cm inner diameter) for a given gas flow rate,  $Q$ , an estimate of the coal particle

density,  $\rho_{\text{coal}}$ , and assuming plug flow. The resulting expression, valid only for  $d_{\text{max}} > 1 \mu\text{m}$  and particle Reynolds numbers ( $\text{Re}_p$ )  $< 1$ , is given by Equation 2.1

$$d_{\text{max}} = 18\mu Q / \rho_{\text{coal}} g A_{\text{impinger}} \quad (2.1)$$

where  $\mu$  is the gas viscosity,  $A_{\text{impinger}}$  is the impinger cross-sectional area and  $g$  is the acceleration due to gravity. For Powder River Basin (PRB) coal,  $\rho_{\text{coal}} \approx 720 \text{ kg/m}^3$ , and 3 lpm of air, the drag force of air is sufficient to overcome the particle weight only for particles less than  $40 \mu\text{m}$ . These considerations allow for more accurate estimation of the coal particle sizes undergoing combustion in the furnace.

## 2.2 Drop-Tube Furnace

A tubular furnace reactor (Lindberg/Blue M, Model HTF55342C,  $T_{\text{max}}=1200^\circ\text{C}$ , ThermoElectron Corp., USA) was used in all experiments. It is also called a “drop-tube” furnace due to its vertical orientation during operation, and it consists of a centered alumina tube (5.72-cm inner diameter and 121.92-cm long) with its wall temperature regulated by electrical resistance heating and two thermocouples located on opposing sides of the tube’s outer wall and at the vertical center of the tube. The furnace temperature was fixed at  $1100^\circ\text{C}$ , which previous measurements have shown to coincide with the tube wall temperature for  $\sim 0.6 \text{ m}$  about the vertical center of the tube. Detailed temperature profile data are included in Appendix A.

## **2.3 Particle Sampling and Collection**

Particles generated during each coal combustion experiment were size-separated into coarse and fine fractions, and the size distribution of fine fraction (submicrometer particles) was measured from a slip-stream flow.

### **2.3.1 Cascade Impactor**

For the duration of each experiment, particles exiting the furnace were first inertially separated and collected using a six-stage cascade impactor (Mark III, Pollution Control System Corp., Seattle, WA) with a final stage 50% cut-off aerodynamic diameter of 0.5  $\mu\text{m}$ . The final-stage cut-off diameter is sufficiently larger than the maximum size of the measured particle size distribution such that particle loss artifacts from non-ideal collection efficiency of the final stage are assumed to be negligible. Particles collected in the cascade impactor are referred to as the coarse fraction.

### **2.3.2 Scanning Mobility Particle Sizer (SMPS)**

Downstream of the cascade impactor, submicrometer particles ( $< 0.5 \mu\text{m}$ ) were sampled in real-time (from a 0.3-lpm slipstream) with a scanning mobility particle sizer (SMPS, TSI Inc., Shoreview, MN) to obtain particle size distributions in the range 9-425 nm.

### **2.3.3 Submicrometer Particle Collection**

All unsampled particles downstream of the cascade impactor were referred to as the fine fraction and collected on Teflon filters for analyses of particle morphology and mineral content and ash composition. The submicrometer particle morphology was determined from micrographs obtained by an FEI Nova 2300 field-emission scanning electron microscope (SEM), and analysis for ash mineral content was performed using a Rigaku Geigerflex D-MAX/A x-ray diffractometer (XRD), the MDI mineral database, and Jade Plus software.

## **2.4 Flue-Gas Sampling**

The filtered flue gas was also sampled during experiments to determine the real-time CO<sub>2</sub> concentration as follows.

### **2.4.1 CO<sub>2</sub> Monitor**

A portable CO<sub>2</sub> analyzer (NOVA Analytical Systems, Inc., Model 302A) was used to monitor the CO<sub>2</sub> volume concentration in the flue gas being exhausted. The analyzer draws 0.9 lpm of flue gas through a condensate removal filter and a secondary filter on to an infrared detector and displays the CO<sub>2</sub> concentration in real-time. The detection range for the instrument is 0-100% CO<sub>2</sub> at 0.1% resolution.

## 2.5 Experiment Test Plan

Table 2.1 is a summary of the experiment test plan for all sets of experiments whose results are discussed in the following chapters. Four sets of experiments were performed and their respective objectives are as follows:

1. To determine the effect of O<sub>2</sub>/coal ratio on submicrometer particle formation in conventional O<sub>2</sub>-N<sub>2</sub> systems (Set I) compared with oxy-combustion O<sub>2</sub>-CO<sub>2</sub> systems (Set II) using Powder River Basin (PRB) coal.
2. To determine the effect of flue gas recycle ratio on submicrometer particle formation during oxy-coal combustion (Set III) using PRB coal.
3. To determine the effect of coal composition on submicrometer particle formation during conventional (air)- and oxy-coal combustion (Set IV) using both American and Chinese coals.

Detailed descriptions of the various coal types listed in Table 2.2 are given in Chapter 5. However, the proximate, ultimate, and mineral analyses for PRB coal are given in Table 2.1.

**Table 2.1 Proximate Analysis, Ultimate Analysis, and Mineral Analysis for Powder River Basin Coal**

Coal Name	Proximate analysis				Ultimate Analysis						Q <sub>net,d</sub> MJ/kg
	M <sub>ad</sub>	Ash <sub>d</sub>	VM <sub>d</sub>	FC <sub>d</sub>	S <sub>d</sub>	C <sub>d</sub>	H <sub>d</sub>	N <sub>d</sub>	O <sub>d</sub>	Cl <sub>d</sub>	
PRB	27.70	8.00	48.30	42.90	0.57	67.30	4.58	0.96	19.92	0.01	28.04
Mineral		SiO <sub>2</sub>	Al <sub>2</sub> O <sub>3</sub>	CaO	Fe <sub>2</sub> O <sub>3</sub>	MgO	K <sub>2</sub> O	Na <sub>2</sub> O	P <sub>2</sub> O <sub>5</sub>	TiO <sub>2</sub>	
Relative % Wt.		37.9	16.1	19.7	5.9	4.9	0.6	1.4	1.7	1.2	
M = Moisture, VM = Volatile Matter, FC - Fixed Carbon											
<sup>ad</sup> air-dried <sup>d</sup> dry, <sup>*</sup> as-received											

Table 2.2 Summary of Experiment Plan

Set	#	Coal Name	System	Furnace Temp. (°C)	Input Flowrate (lpm)	Recycle Flowrate (lpm)	Recycle Ratio (vol.%)	O <sub>2</sub> Flowrate (lpm)	N <sub>2</sub> or CO <sub>2</sub> Flowrate (lpm)	Inlet O <sub>2</sub> Conc.	Inlet CO <sub>2</sub> Conc.	O <sub>2</sub> /Coal Ratio (mol/mol)	Objective	
I	1	PRB	O <sub>2</sub> /N <sub>2</sub>	1100	3.0	0	0%	0.15	2.85	5.00%	95.00%	3.14	To determine the effect of O <sub>2</sub> /coal ratio on submicrometer particle formation in conventional O <sub>2</sub> -N <sub>2</sub> systems (Set I) compared with oxy-coal O <sub>2</sub> -CO <sub>2</sub> systems (Set II)	
	2							0.30	2.70	10.00%	90.00%	6.28		
	3							0.60	2.40	20.00%	80.00%	12.6		
	4							0.90	2.10	30.00%	70.00%	18.8		
	5							1.20	1.80	40.00%	60.00%	25.1		
	6							1.50	1.50	50.00%	50.00%	31.4		
II	1	PRB	O <sub>2</sub> /CO <sub>2</sub>	1100	3.0	0	0%	0.60	2.40	20.00%	80.00%	12.6		
	2							0.90	2.10	30.00%	70.00%	18.8		
	3							1.20	1.80	40.00%	60.00%	25.1		
	4							1.50	1.50	50.00%	50.00%	31.4		
III	1	PRB	O <sub>2</sub> /CO <sub>2</sub>	1200	3.0	0	0%	0.60	2.40	20.00%	80.00%	12.6		To determine the effect of flue gas recycle ratio on submicrometer particle formation during oxy-coal combustion (Set III)
	2				2.4	0.6	20%	0.48	1.92	19.90%	80.10%	12.5		
	3				1.8	1.2	40%	0.36	1.44	19.79%	80.21%	12.4		
	4				1.2	1.8	60%	0.24	0.96	19.67%	80.33%	12.3		
	5				0.6	2.4	80%	0.12	0.48	19.53%	80.47%	12.3		
IV	1	PRB	O <sub>2</sub> /N <sub>2</sub> (air)	1100	3.0	0	0%	0.6	2.4	20%	80%	12.6	To determine the effect of coal composition on submicrometer particle formation during conventional (air)- and oxy-coal combustion (Set IV)	
	2	IL#6												
	3	S01												
	4	S04												
	5	S07												
	6	S10												
	7	PRB	O <sub>2</sub> /CO <sub>2</sub>		1.8	1.2	40%	0.36	1.44	20%	80%	12.4		
	8	IL#6												
	9	S01												
	10	S04												
	11	S07												
	12	S10												

## Chapter 3

# Effect of O<sub>2</sub>/Coal Ratio on Submicrometer Particle Formation during Oxy-Combustion

The oxidizer/fuel ratio is a common parameter in combustion, and the effect of varying the O<sub>2</sub>/coal ratio was investigated to clarify the key roles of bulk gas composition during char burning and submicrometer particle formation. The bulk gas composition was used to estimate the adiabatic flame temperature of burning char particles. The char surface temperatures were then used to estimate the vaporization rates of volatile metals from burning char particles. The bulk gas composition also has direct and indirect effects on the vapor equilibria of metal-oxide reduction into volatile metals and sub-oxides: directly via the partial pressures of bulk O<sub>2</sub> and CO<sub>2</sub> and indirectly via their effect on the adiabatic flame temperature and therefore the temperature-dependent equilibrium constants for metal-oxide reduction.

### 3.1 Effect of Flame Temperature

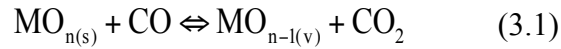
Based on thermochemical considerations alone, metal and metal-oxide vaporization rates exhibit strong dependence on temperature. Char surface temperatures during

burnout were therefore estimated for each combustion condition. These temperatures were assumed to be the respective adiabatic flame temperatures, using the widely used chemical equilibrium computer code, STANJAN<sup>53</sup>, since vaporization occurs from the char surface. The coal-O<sub>2</sub>-CO<sub>2</sub> or coal-O<sub>2</sub>-N<sub>2</sub> mixture compositions for each combustion condition were used to estimate the adiabatic flame temperatures for the burning char, and the corresponding temperatures for each reactant mixture are included in Table 3.1.

**Table 3.1 Estimates of Adiabatic Flame Temperature for Varied O<sub>2</sub>/Coal Ratios in Coal-O<sub>2</sub>/N<sub>2</sub> and Coal-O<sub>2</sub>/CO<sub>2</sub> Systems**

Set	#	Reactant System	O <sub>2</sub> Flowrate (lpm)	N <sub>2</sub> or CO <sub>2</sub> Flowrate (lpm)	O <sub>2</sub> Vol. Conc.	N <sub>2</sub> or CO <sub>2</sub> Vol. Conc.	O <sub>2</sub> /Coal Ratio (mol/mol)	T <sub>ad</sub> (K)
I	1	Coal-O <sub>2</sub> /N <sub>2</sub>	0.15	2.85	5%	95%	3.14	1551
	2		0.30	2.70	10%	90%	6.28	1549
	3		0.60	2.40	20%	80%	12.6	1547
	4		0.90	2.10	30%	70%	18.8	1546
	5		1.20	1.80	40%	60%	25.1	1545
	6		1.50	1.50	50%	50%	31.4	1544
II	1	Coal-O <sub>2</sub> /CO <sub>2</sub>	0.60	2.40	20%	80%	12.6	1490
	2		0.90	2.10	30%	70%	18.8	1495
	3		1.20	1.80	40%	60%	25.1	1500
	4		1.50	1.50	50%	50%	31.4	1506
Total flow rate = 3 lpm, coal feed rate = 2 g/hr								
Furnace temperature = 1100 °C								

The reduction of metal-oxides ( $\text{MO}_n$ ) by CO into more volatile metals and sub-oxides ( $\text{MO}_{n-1}$ ) was assumed to be at equilibrium at the surface of burning char particles, as done by Suriyawong *et al.*<sup>30</sup> and given by the reaction in Equation 3.1.



To obtain reasonable estimates of the equilibrium constants for such reactions, Senior *et al.*<sup>48</sup> fit experimental data (over the range 1500-2500 K) using the temperature-dependent expression of Equation 3.2.

$$\ln(K_i) = A_i + (B_i \times 10^4)/T \quad (3.2)$$

where  $K_i$  is the equilibrium constant for a metal oxide (atm),  $A_i$  and  $B_i$  are respective coefficients, and  $T$  is the vaporization temperature (K). Table 3.2 is a summary of the equilibrium constant coefficients for vaporization reactions of typical metal oxides present in coals.

**Table 3.2 Equilibrium Constant Coefficients for Vaporization Reactions of Typical Metal Oxides in Coals<sup>48</sup>**

Vaporization Reaction	A	B
$\text{SiO}_2 + \text{CO} \rightleftharpoons \text{SiO} + \text{CO}_2$	18.8256	-5.9700
$\text{Al}_2\text{O}_3 + \text{CO} \rightleftharpoons \text{Al}_2\text{O} + \text{CO}_2$	24.0505	-11.3361
$\text{CaO} + \text{CO} \rightleftharpoons \text{Ca} + \text{CO}_2$	13.2182	-6.1507
$\text{MgO} + \text{CO} \rightleftharpoons \text{Mg} + \text{CO}_2$	14.4976	-5.4094
$\text{FeO} + \text{CO} \rightleftharpoons \text{Fe} + \text{CO}_2$	11.4942	-4.2064

Equilibrium constants for sub-oxides listed in the vaporization reactions above were then estimated at calculated flame temperatures, according to Equation 3.2, for each combustion condition and summarized in Table 3.3.

**Table 3.3 Calculated Equilibrium Constants for Metal-Oxide Reduction during Varied O<sub>2</sub>/Coal Ratios in Coal-O<sub>2</sub>/N<sub>2</sub> and Coal-O<sub>2</sub>/CO<sub>2</sub> Systems**

Set	#	Reactant System	T <sub>ad</sub> (K)	K [SiO, atm]	K [Al <sub>2</sub> O, atm]	K [Ca, atm]	K [Mg, atm]	K [Fe, atm]
I	1	Coal-O <sub>2</sub> /N <sub>2</sub>	1551	2.85E-09	4.95E-22	3.26E-12	1.40E-09	1.62E-07
	2		1549	2.75E-09	4.63E-22	3.15E-12	1.35E-09	1.58E-07
	3		1547	2.62E-09	4.22E-22	2.99E-12	1.29E-09	1.53E-07
	4		1546	2.53E-09	3.95E-22	2.88E-12	1.25E-09	1.49E-07
	5		1545	2.45E-09	3.73E-22	2.80E-12	1.22E-09	1.46E-07
	6		1544	2.40E-09	3.57E-22	2.73E-12	1.20E-09	1.44E-07
II	1	Coal-O <sub>2</sub> /CO <sub>2</sub>	1490	5.94E-10	2.52E-23	6.48E-13	3.37E-10	5.38E-08
	2		1495	6.77E-10	3.23E-23	7.42E-13	3.80E-10	5.90E-08
	3		1500	7.78E-10	4.20E-23	8.56E-13	4.31E-10	6.50E-08
	4		1506	9.07E-10	5.62E-23	1.00E-12	4.95E-10	7.24E-08
Total flow rate = 3 lpm, coal feed rate = 2 g/hr								
Furnace temperature = 1100 °C								

Table 3.3 reveals the relative volatility of the sub-oxides from metal-oxide reduction at estimated flame temperatures. For instance, SiO and Fe have the highest equilibrium constants at each condition.

## **3.2 Effect of Gas Composition**

One principal effect of gas composition on submicrometer particle formation is through the effect on vapor equilibria of metal-oxide reduction into volatile metals and sub-oxides, as given in Equation 3.1. However the exact equilibrium relations differ between the coal-O<sub>2</sub>-N<sub>2</sub> system and the coal-O<sub>2</sub>-CO<sub>2</sub> system because, in the former case, the only source of CO<sub>2</sub> at the char surface is that which is evolved during the metal-oxide reduction reaction. As such, these two cases are treated separately and are as follows.

### 3.2.1 Coal-O<sub>2</sub>-N<sub>2</sub> System

The equilibrium constant  $K_i$  for the metal oxides that undergo the reduction reaction of Equation 3.2 is given by Equation 3.3.

$$K_i = \frac{p_{MO_{n-1}} p_{CO_2}}{a_{MO_n} p_{CO}} \quad (3.3)$$

where  $p_i$  is the partial pressure of species  $i$  and,  $a_{MO_n}$ , the activity of the solid metal oxide is assumed to be equal to 1, while  $p_{CO_2}$  is equal to  $p_{MO_{n-1}}$  since the only source

of CO<sub>2</sub> at the char surface is that generated during the evolution of metal or sub-oxide vapor, MO<sub>n-1</sub>, resulting in Equation 3.4 for O<sub>2</sub>-N<sub>2</sub> systems.

$$K_i = \frac{P_{MO_{n-1}}^2}{P_{CO}} \quad (3.4)$$

Assuming all the O<sub>2</sub> reaching the char surface is consumed and CO is the only product, the partial pressure of CO at the char surface is given by Equation 3.5 in the Langmuir-adsorption form of Senior *et al.*<sup>48</sup>

$$p_{CO}(\text{at surface}) = \frac{2P_{O_2(\text{bulk})}}{1 + P_{O_2(\text{bulk})}} \quad (3.5)$$

The partial pressure of the volatile sub-oxides can then be expressed as a function of the temperature-dependent equilibrium constant and the bulk O<sub>2</sub> concentration by combining Equations 3.4 and 3.5 to give Equation 3.6

$$P_{MO_{n-1}} = \left[ \frac{2P_{O_2(\text{bulk})}}{1 + P_{O_2(\text{bulk})}} \cdot K_i(T) \right]^{1/2} \quad (3.6)$$

### 3.2.2 Coal-O<sub>2</sub>-CO<sub>2</sub> System

In this system, in addition to the CO<sub>2</sub> at the char surface generated by the reduction of metal oxides, diluent CO<sub>2</sub> also contributes to the CO<sub>2</sub> concentration at the char surface. As such, the expression for the equilibrium constant is given by Equation 3.3 as in the O<sub>2</sub>-N<sub>2</sub> system. However, in this case, CO<sub>2</sub> is not only produced during the evolution of sub-oxide vapors, but it also exists in the bulk gas mixture. Equation 3.3 can then be combined with Equation 3.5, as before, to obtain the partial pressure for volatile sub-oxides, as shown in Equation 3.7.

$$P_{MO_{n-1}} = \frac{2p_{O_2(bulk)}}{P_{CO_2}(1 + p_{O_2(bulk)})} \cdot K_i(T) \quad (3.7)$$

The bulk gas concentrations, whether O<sub>2</sub> (in the O<sub>2</sub>-N<sub>2</sub> system) or O<sub>2</sub> and CO<sub>2</sub> (in the O<sub>2</sub>-CO<sub>2</sub> system), can therefore be used to estimate the amount of particular sub-oxides generated and the total amount of solid metal-oxides vaporized via the chemical reduction pathway.

## 3.3 Heat & Mass Transport Considerations

The replacement of N<sub>2</sub> with CO<sub>2</sub> also has important heat and mass transfer implications because the physical properties of N<sub>2</sub> and CO<sub>2</sub> are significantly different. The larger specific heat capacity of CO<sub>2</sub> (1.7x larger) compared to N<sub>2</sub>

results in marked decreases in furnace gas temperatures, reduced char burnout rates, and decreased char surface temperatures by up to  $500^{\circ}\text{C}$ <sup>54, 55</sup>, as well as delayed ignition times for coal particles and char particles<sup>56, 57</sup>.

Since the char burning process is diffusion-limited, the mass diffusivity of  $\text{O}_2$  from the bulk to the char surface is also an important quantity. The mass diffusivity of  $\text{O}_2$  in  $\text{CO}_2$  is less than the diffusivity of  $\text{O}_2$  in  $\text{N}_2$ , so that the rates of char oxidation and the accompanying heat generation are retarded when  $\text{N}_2$  is replaced with  $\text{CO}_2$ . Also, the heat and mass transport effects are coupled in that the mass diffusivity is a function of local temperature, and lower char surface temperatures during

oxy-combustion that arise due to thermochemical and heat transport considerations can reduce the local gas temperatures in the vicinity of the char particle enough to further impede  $\text{O}_2$  transport to the char surface.

### **3.4 Results and Discussion**

Powder River Basin (PRB) subbituminous coal, whose characteristics will be described in more detail in Chapter 5, was combusted to demonstrate the effects of flame temperature and bulk gas composition on submicrometer particle formation. Table 3.4 contains calculated partial pressures of sub-oxides generated from metal-

oxides contained in PRB coal at the flame temperatures corresponding to the bulk gas mixtures delineated in Table 3.1.

**Table 3.4 Calculated Sub-Oxide and Metal Partial Pressures from Metal-Oxide Reduction during Varied O<sub>2</sub>/Coal Ratios in Coal-O<sub>2</sub>/N<sub>2</sub> and Coal-O<sub>2</sub>/CO<sub>2</sub> Systems**

Set	#	Reactant System	T <sub>ad</sub> (K)	<i>p</i> [SiO, atm]	<i>p</i> [Al <sub>2</sub> O, atm]	<i>p</i> [Ca, atm]	<i>p</i> [Mg, atm]	<i>p</i> [Fe, atm]
I	1	Coal-O <sub>2</sub> /N <sub>2</sub>	1551	1.65E-05	6.87E-12	5.57E-07	1.15E-05	1.24E-04
	2		1549	2.24E-05	9.18E-12	7.57E-07	1.57E-05	1.70E-04
	3		1547	2.96E-05	1.19E-11	9.98E-07	2.08E-05	2.26E-04
	4		1546	3.42E-05	1.35E-11	1.15E-06	2.41E-05	2.62E-04
	5		1545	3.75E-05	1.46E-11	1.26E-06	2.64E-05	2.89E-04
	6		1544	4.00E-05	1.54E-11	1.35E-06	2.82E-05	3.10E-04
II	1	Coal-O <sub>2</sub> /CO <sub>2</sub>	1490	2.47E-10	1.05E-23	2.70E-13	1.41E-10	2.24E-08
	2		1495	4.47E-10	2.13E-23	4.89E-13	2.51E-10	3.89E-08
	3		1500	7.41E-10	4.00E-23	8.15E-13	4.10E-10	6.19E-08
	4		1506	1.21E-09	7.50E-23	1.34E-12	6.60E-10	9.66E-08

The same O<sub>2</sub>-N<sub>2</sub> or O<sub>2</sub>-CO<sub>2</sub> gas concentrations as used in the foregoing calculations were used in combustion experiments with PRB coal. The resulting submicrometer particle size distributions for PRB coal combusted in O<sub>2</sub>-N<sub>2</sub> and PRB coal in O<sub>2</sub>-CO<sub>2</sub> are shown in Figures 3.1 and 3.2 respectively, while the summary statistics for these conditions are in Table 3.5.

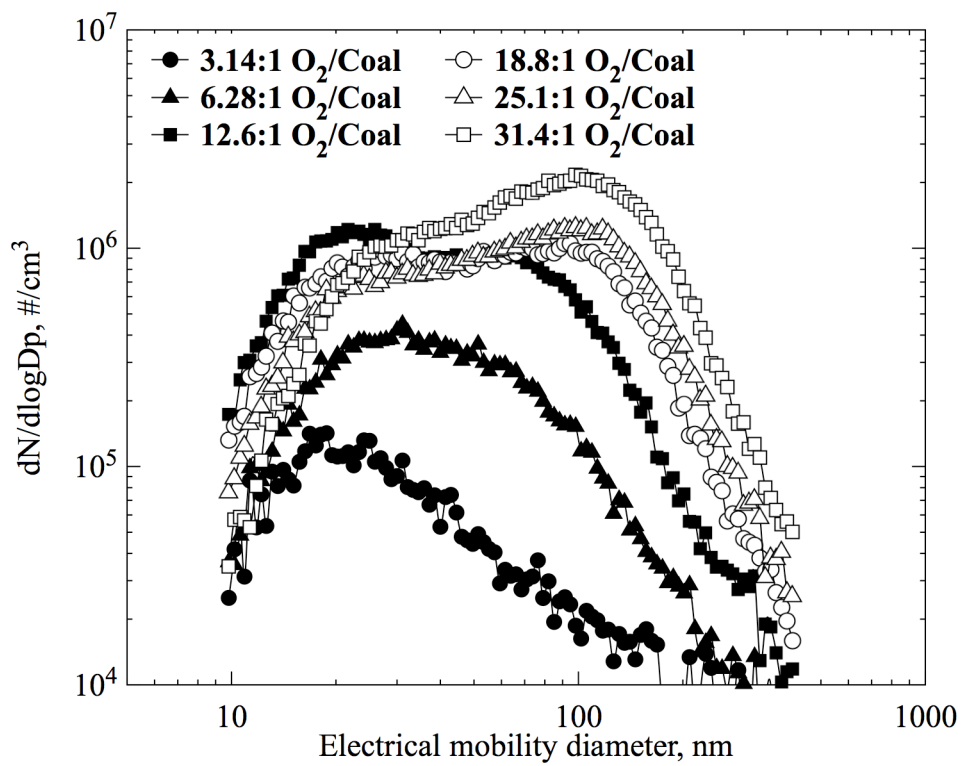


Figure 3.1 Submicrometer Particle Size Distributions during Combustion of PRB Coal Varied O<sub>2</sub>/Coal Ratios in O<sub>2</sub>-N<sub>2</sub> Mixtures

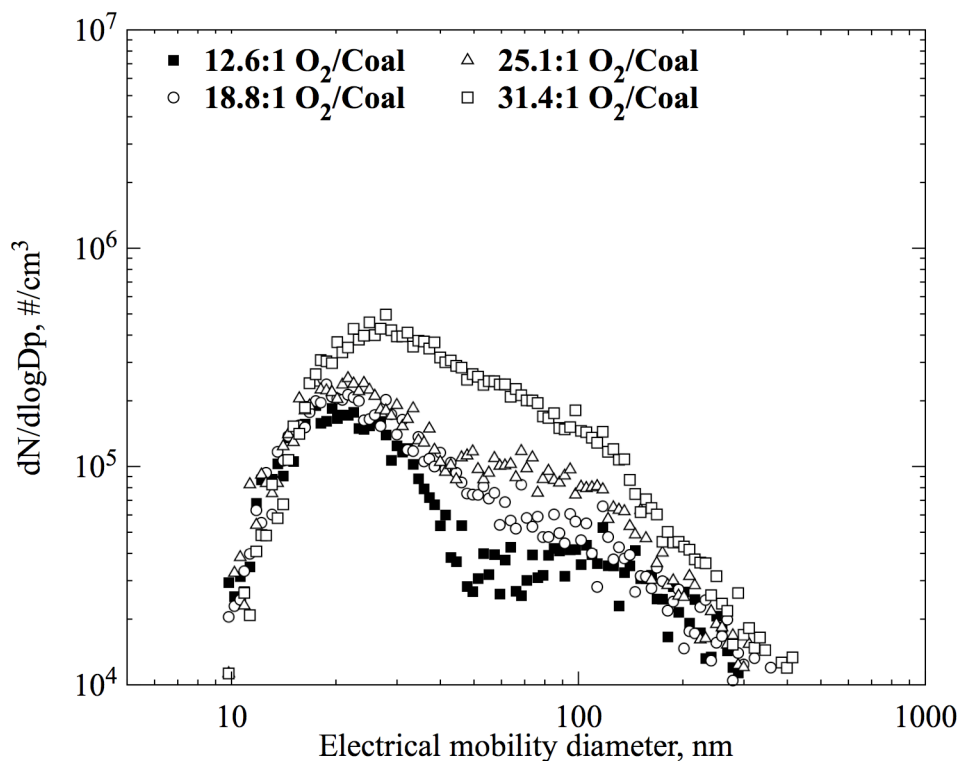


Figure 3.2 Submicrometer Particle Size Distributions during Combustion of PRB Coal with Varied O<sub>2</sub>/Coal Ratios in O<sub>2</sub>-CO<sub>2</sub> Mixtures

Table 3.5 Summary Statistics for Submicrometer Particle Size Distributions during Combustion of PRB Coal with Varied O<sub>2</sub>/Coal Ratios

Set	#	Reactant System	O <sub>2</sub> Vol. Conc.	O <sub>2</sub> /Coal Ratio (mol/mol)	T <sub>ad</sub> (K)	N <sub>total</sub> (#/cm <sup>3</sup> )	d <sub>pg</sub> (nm)	σ <sub>g</sub>	A <sub>total</sub> (nm <sup>2</sup> /cm <sup>3</sup> )	V <sub>total</sub> (nm <sup>3</sup> /cm <sup>3</sup> )
I	1	Coal-O <sub>2</sub> /N <sub>2</sub>	5%	3.14	1516.6	7.88 x 10 <sup>4</sup>	29.8	2.1	9.75 x 10 <sup>8</sup>	3.36 x 10 <sup>10</sup>
	2		10%	6.28	1865.9	2.88 x 10 <sup>5</sup>	38.0	1.9	3.33 x 10 <sup>9</sup>	8.21 x 10 <sup>10</sup>
	3		20%	12.6	1857.9	9.49 x 10 <sup>5</sup>	37.7	2.0	1.22 x 10 <sup>10</sup>	2.73 x 10 <sup>11</sup>
	4		30%	18.8	1852.1	9.81 x 10 <sup>5</sup>	49.2	2.2	2.15 x 10 <sup>10</sup>	5.47 x 10 <sup>11</sup>
	5		40%	25.1	1847.4	1.03 x 10 <sup>6</sup>	59.7	2.1	3.02 x 10 <sup>10</sup>	8.15 x 10 <sup>11</sup>
	6		50%	31.4	1843.5	1.58 x 10 <sup>6</sup>	69.2	2.0	5.49 x 10 <sup>10</sup>	1.53 x 10 <sup>12</sup>
II	1	Coal-O <sub>2</sub> /CO <sub>2</sub>	20%	12.6	1606.4	1.00 x 10 <sup>5</sup>	32.3	2.3	1.86 x 10 <sup>9</sup>	6.35 x 10 <sup>10</sup>
	2		30%	18.8	1627.3	1.26 x 10 <sup>5</sup>	34.1	2.2	2.18 x 10 <sup>9</sup>	7.13 x 10 <sup>10</sup>
	3		40%	25.1	1650.0	1.55 x 10 <sup>5</sup>	36.8	2.2	2.74 x 10 <sup>9</sup>	8.14 x 10 <sup>10</sup>
	4		50%	31.4	1674.7	2.82 x 10 <sup>5</sup>	40.9	2.0	4.84 x 10 <sup>9</sup>	1.40 x 10 <sup>11</sup>
Total flow rate = 3 lpm, coal feed rate = 2 g/hr										
Furnace temperature = 1100 °C										

With a fixed furnace temperature and residence time for all tests, the total time available for coagulation and condensation growth was maintained for all conditions, so that the size distribution statistics in Table 3.5 can be more readily related to the calculated sub-oxide partial pressures in Table 3.4. In both conventional ( $O_2-N_2$ ) and oxy-combustion ( $O_2-CO_2$ ) systems, the geometric mean size, total number concentration, total surface area concentration, and total volume concentration all increase with increasing  $O_2$ /coal ratio due to enhanced vaporization rates and oxidation rates of sub-oxides to form metal oxide particles. As predicted by the vaporization-chemical nucleation pathway and equilibrium considerations, at a given  $O_2$ /coal ratio, the total number concentration, surface area concentration, and volume concentration are all higher in the conventional ( $O_2-N_2$ ) system than in the oxy-combustion ( $O_2-CO_2$ ) system. This can be explained by the difference in metal oxide vaporization rates due to the effects of flame temperature, gas composition, and heat & mass transport properties as describe above and confirmed by other studies<sup>30, 45, 58</sup> Figure 3.3 also highlights the significant positive correlation between the total sub-oxide partial pressures calculated\* and the measured total volume concentrations during oxy-combustion, demonstrating that the vaporization-nucleation pathway, as described by the foregoing expressions, can account for the submicrometer particles observed during experiments in  $O_2-CO_2$  systems.

---

\* The plotted values of total sub-oxide partial pressure are weighted sums over the sub-oxides of Table 3.4, with respect to the mineral metal-oxide composition of PRB coal.

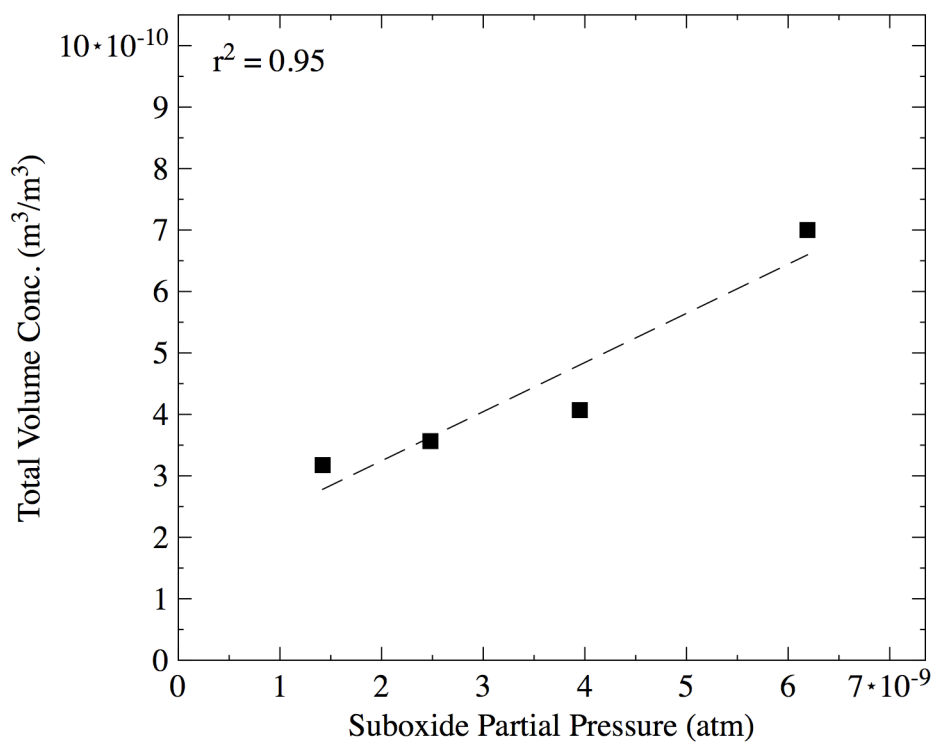


**Figure 3.3 Scatter Plot of Total Volume Concentrations for Submicrometer Particles Sampled vs. Calculated Total Sub-Oxide Partial Pressures during Oxy-Coal Combustion at Varied O<sub>2</sub>/Coal Ratios**

## Chapter 4

# Role of Flue-Gas Recycle in Submicrometer Particle Formation during Oxy-Combustion

Oxy-coal combustion involves the removal of  $N_2$  from air in the combustion process in order to increase the  $CO_2$  concentration in flue gas from  $\sim 16\%$  to  $\sim 98\%$  and therefore avoid costly gas separation processes required prior to  $CO_2$  storage. Flue-gas recycle is a feature of oxy-coal combustion that uses  $CO_2$ -rich flue gas as a replacement for  $N_2$  to moderate temperatures in PC boilers while coal burns in  $O_2$ . Clearly, this combustion modality significantly alters the bulk gas composition in all parts of oxy-combustion systems, including in a drop-tube furnace setup during oxy-coal combustion. Thus, to quantify the effect of flue-gas recycle on submicrometer particle formation, it is necessary to estimate the effect of flue-gas recycle on bulk gas compositions throughout the drop-tube furnace setup during steady-state operation.

## **4.1 Effect of Flue-Gas Recycle on Gas Composition**

The flue-gas recycle ratio is the ratio of the recycled flue gas volume flow rate to the total flow rate through the furnace, and changes in the bulk gas composition affect char burnout and submicrometer particle formation. Hence, it was necessary to determine the effect of flue-gas recycle ratio on the CO<sub>2</sub> concentrations throughout the system. Assuming complete char burnout, mass and mole balances were performed over all gas streams in the drop-tube furnace system to estimate the CO<sub>2</sub> mole fractions throughout the system for each oxy-coal combustion condition (see Appendix C for detailed balance calculations).

### **4.1.1 System Mole Balances for CO<sub>2</sub>**

The inlet concentration of CO<sub>2</sub> into the drop-tube furnace was determined during steady-state operation with flue-gas recycle by applying mole balances at all gas splitting and combination points in the system and accounting for all gas streams. Figure 4.1 is a system schematic illustrating the gas mixture states accounted for in the balance calculations.

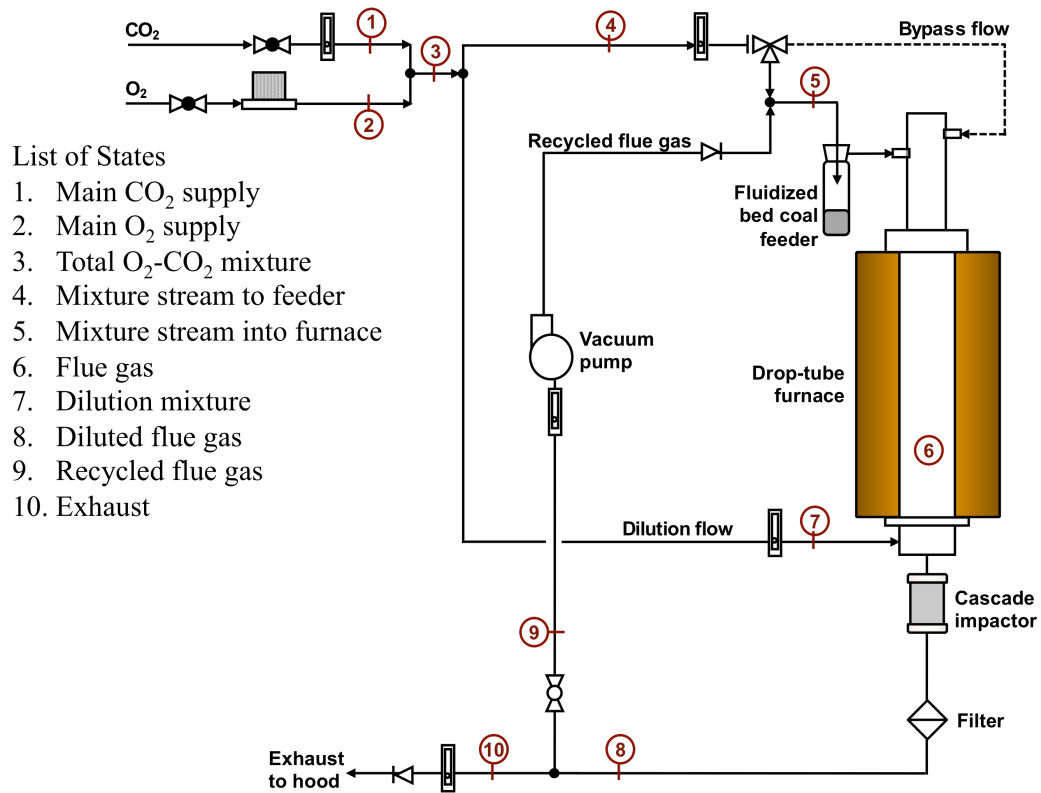


**Figure 4.1 Drop-Tube Furnace Setup with Gas Mixture States during Steady Oxy-Combustion Operation**

The CO<sub>2</sub> concentration at the furnace inlet was then expressed in terms of known, measured quantities, as shown in Equation 4.1

$$x_5 = \frac{x_4 F_4 + x_8 F_9}{F_5} \quad (4.1)$$

where  $x_i$  and  $F_i$  are the CO<sub>2</sub> mole fraction (or volume fraction) and volumetric flow rate at state  $i$ , respectively.

The calculated CO<sub>2</sub> mole fractions at the system exhaust were compared to online measurements of the CO<sub>2</sub> volume fraction at the exhaust using a portable infrared CO<sub>2</sub> gas monitor (Nova Scientific) and found to be in good agreement. The CO<sub>2</sub> concentration at the furnace inlet was found to increase only slightly with increasing recycle ratio, from 80% at no-recycle to 80.47% at 80% recycle. Figure 4.2 is a plot of CO<sub>2</sub> concentration at the furnace inlet and corresponding adiabatic flame temperatures as a function of flue-gas recycle ratio.

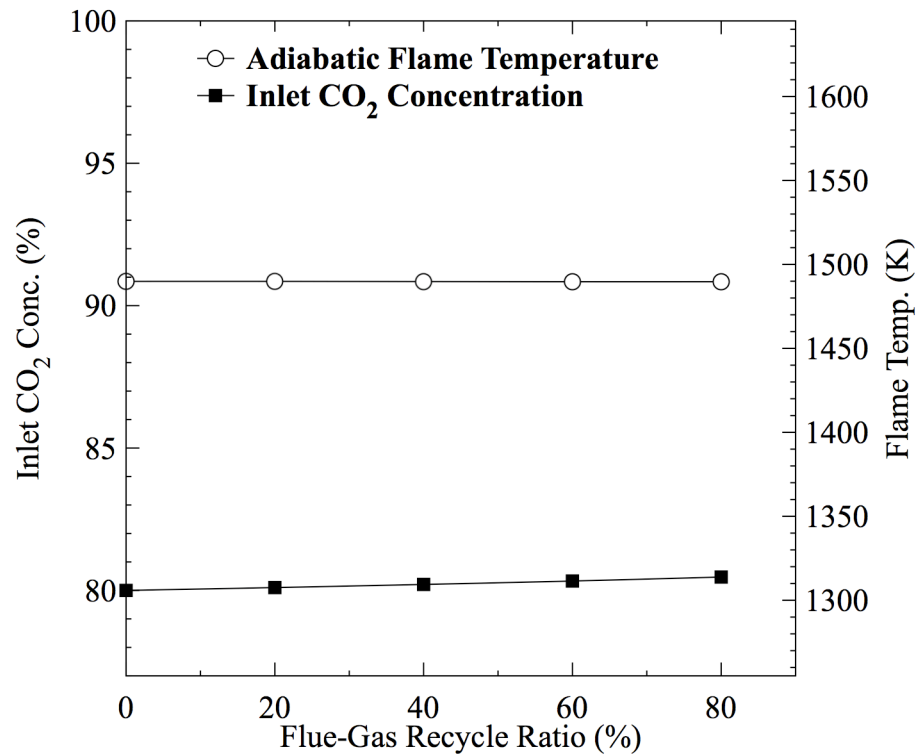


**Figure 4.2 CO<sub>2</sub> Concentrations at Furnace Inlet and Adiabatic Flame Temperatures as a Function of Flue-Gas Recycle Ratio**

## 4.2 Results and Discussion

The submicrometer particle size distributions obtained during oxy-combustion of PRB coal with varied flue-gas recycle ratios are shown in Figure 4.3\*, and the size distribution summary statistics are given in Table 4.1.

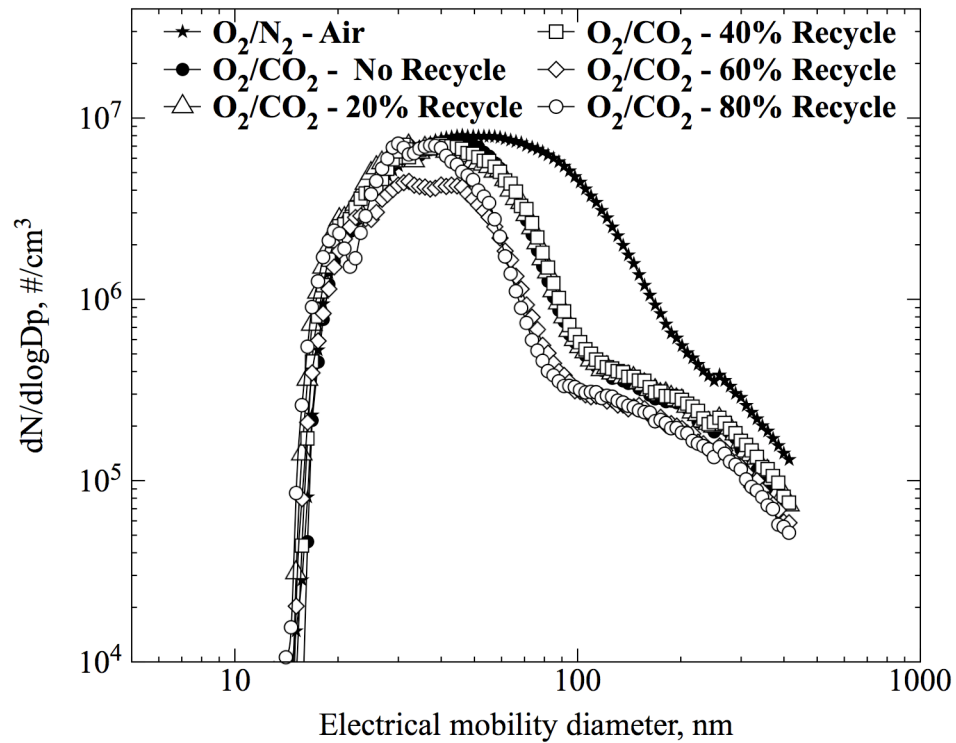


**Figure 4.3 Submicrometer Particle Size Distributions for Conventional Coal-Air Combustion and Oxy-Combustion at Varied Flue-Gas Recycle Ratios for PRB Coal**

---

\*The total gas flow rate through the furnace (and therefore the residence time) during all oxy-combustion experiments, with and without flue-gas recycle, was kept fixed at 3 lpm (40-sec residence time). While initiating flue-gas recycle, the same amount of recycle volume flow was applied as a turndown of the supply gases from the laboratory gas cylinders.

**Table 4.1 Summary Statistics for Submicrometer Particle Size Distributions during Combustion of PRB Coal with Varied Flue-Gas Recycle Ratios at 1200 °C Furnace Temperature**

Set	#	Input Flowrate (lpm)	Input Gas Composition	O <sub>2</sub> /Coal Ratio (mol/mol)	N <sub>total</sub> (#/cm <sup>3</sup> )	d <sub>pg</sub> (nm)	σ <sub>g</sub>	A <sub>total</sub> (nm <sup>2</sup> /cm <sup>3</sup> )	V <sub>total</sub> (nm <sup>3</sup> /cm <sup>3</sup> )
III	1	3.0	O <sub>2</sub> /N <sub>2</sub> (air)	13.2	5.15 x 10 <sup>6</sup>	54.3	1.7	9.94 x 10 <sup>10</sup>	2.42 x 10 <sup>12</sup>
	2	3.0	O <sub>2</sub> /CO <sub>2</sub> (with no recycle)	12.6	3.43 x 10 <sup>6</sup>	42.8	1.6	2.57 x 10 <sup>10</sup>	7.14 x 10 <sup>11</sup>
	3	2.4	O <sub>2</sub> /CO <sub>2</sub> (with 20% recycle)	12.5	3.45 x 10 <sup>6</sup>	41.7	1.7	4.11 x 10 <sup>10</sup>	1.01 x 10 <sup>12</sup>
	4	1.8	O <sub>2</sub> /CO <sub>2</sub> (with 40% recycle)	12.4	3.46 x 10 <sup>6</sup>	42.8	1.6	4.17 x 10 <sup>10</sup>	1.05 x 10 <sup>12</sup>
	5	1.2	O <sub>2</sub> /CO <sub>2</sub> (with 60% recycle)	12.3	2.07 x 10 <sup>6</sup>	40.0	1.7	4.32 x 10 <sup>10</sup>	1.09 x 10 <sup>12</sup>
	6	0.6	O <sub>2</sub> /CO <sub>2</sub> (with 80% recycle)	12.3	2.74 x 10 <sup>6</sup>	38.0	1.6	2.75 x 10 <sup>10</sup>	6.97 x 10 <sup>11</sup>

Increasing flue-gas recycle ratios have the modest effect of increasing the inlet CO<sub>2</sub> concentration and thereby reducing the O<sub>2</sub>/coal ratio from 12.6 (no recycle) to 12.3 (80% recycle). As a result, the geometric mean size decreased from 42.8 nm to 38 nm, while the total number, surface area, and volume concentrations did not vary significantly with flue-gas recycle. However, the differences between oxy-combustion and conventional combustion in air remain—particularly in terms of the geometric mean size and geometric standard deviation, both of which are higher in the case of coal-air combustion than in the case of oxy-coal combustion with or without recycle. This difference may be attributed to the suppressive effect of CO<sub>2</sub> (compared to N<sub>2</sub>) on vaporization rates of volatile metal species and metal oxides,

via its role in determining the char surface temperature during burning and its role in shifting volatile sub-oxide equilibria as discussed in Chapter 3.

Figure 4.4 contains x-ray diffractograms of submicrometer ash samples resulting from PRB coal combustion (a) in air, (b) in  $O_2$ - $CO_2$  without flue-gas recycle, and (c) in  $O_2$ - $CO_2$  with 40% flue-gas recycle.

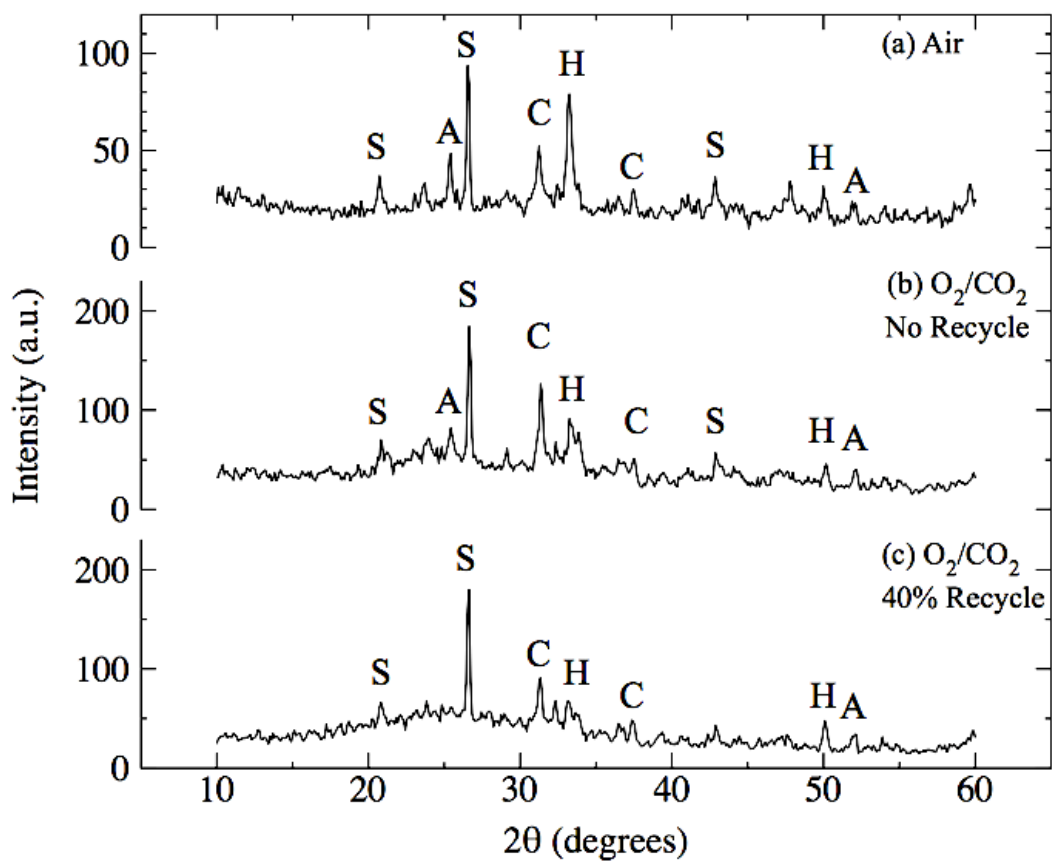


Figure 4.4 X-Ray Diffractograms of Submicrometer Particles Collected during Combustion of PRB Coal at Three Different Conditions (S:  $SiO_2$ , A:  $Al_2O_3$ , C:  $CaO$ , H:  $Fe_2O_3$ )

The XRD detected most of the metal oxides expected to be contained in the submicrometer ash, including silica ( $\text{SiO}_2$ ), calcium oxide ( $\text{CaO}$ ), and iron (III) oxide ( $\text{Fe}_2\text{O}_3$ ). The sample from conventional coal-air combustion appears to have these species most manifest, as expected from the equilibrium calculations with the adiabatic flame temperature. Also, as expected, diffractograms (b) and (c) from the oxy-combustion cases appear to be very similar, barring the slight diminution of  $\text{CaO}$  and  $\text{Fe}_2\text{O}_3$  peak intensities, and confirming that flue-gas recycle has mainly the effect of lowering the adiabatic flame temperature, which has consequent effects on coal devolatilization, the temperature-time history of char burnout, mineral transformations, and vaporization of metals and metal oxides.

# Chapter 5

## Effect of Coal Composition on Submicrometer Particle Formation during Oxy-Combustion

The diversity and heterogeneity of coals plays a significant role in the burning behavior of coal particles and the formation of submicrometer particles. The phenomenological and thermophysical aspects of coal devolatilization, char burning, and pollutant formation have been well-documented for conventional PC combustion as well as for oxy-combustion conditions of different coal seams<sup>23, 31, 34, 58-61</sup>. However, none of the studies reported the effect of flue-gas recycle on submicrometer particle formation across a variety of different coal seams and ranks. Here, two American and four Chinese coals are selected for study.

### 5.1 Coal Sample Selection

Coals from the United States and China were selected due to their primacy in global coal consumption for electricity generation. The two American coals were selected for this work: Powder River Basin (PRB) coal and Illinois #6 coal. Each is being actively used in Ameren UE power plants servicing Missouri and Southern Illinois,

and their ASTM ranks (subbituminous and bituminous) constitute 90% (37% and 53%, respectively) of the coal reserves in the United States<sup>62</sup>. Powder River Basin (PRB) coal is a major source of coal for electric utilities in the U.S. due to its relatively low cost and very low sulfur content, while Illinois #6 coal, in addition to having a higher calorific value and being available due to proximity, is used where SO<sub>2</sub> can be adequately controlled. The four Chinese coals were chosen based on their relative diversity in rank—one of each major ASTM rank.

### 5.1.1 American Coals

PRB coal is typically subbituminous, while the Illinois #6 sample is a high-volatile C bituminous coal. Both coals were obtained from mines owned by Peabody Energy: North Antelope/Rochelle mine (Wright, WY) and Gateway mine (Coulterville, IL), respectively. Table 5.2 contains the proximate and ultimate analyses for the two selected coals, and Table 5.1 contains the mineral content analyses for each coal (supplied for these samples by Ameren UE and Peabody Energy, respectively).

**Table 5.1 Mineral Fractions in Ash Content of Powder River Basin (PRB) and Illinois #6 Coal Samples (Analyses from Ameren UE and Peabody Energy respectively.)**

Coal Name	Mineral Fractions (% wt Relative to Ash Content)								
	SiO <sub>2</sub>	Al <sub>2</sub> O <sub>3</sub>	CaO	Fe <sub>2</sub> O <sub>3</sub>	MgO	K <sub>2</sub> O	Na <sub>2</sub> O	P <sub>2</sub> O <sub>5</sub>	TiO <sub>2</sub>
PRB	37.9	16.1	19.7	5.9	4.9	0.6	1.4	1.7	1.2
IL#6	51.4	20.0	3.8	16.3	0.9	2.1	1.2	0.2	1.0

## 5.1.2 Chinese Coals

Four Chinese coals were selected based on their ASTM rank as follows: S01 (lignite), S04 (anthracite), S07 (subbituminous), and S10 (bituminous). The lignite, subbituminous, and bituminous samples were obtained from mines in Inner Mongolia Province, while the anthracite sample (S04) was obtained from a mine in Chongqing Province. Table 5.2 contains the proximate and ultimate analyses for each of the four selected coals.

**Table 5.2 Proximate and Ultimate Analyses for American & Chinese Coals**

Coal Name	Proximate analysis				Ultimate Analysis						Q <sub>net,d</sub> MJ/kg
	M <sub>ad</sub>	Ash <sub>d</sub>	VM <sub>d</sub>	FC <sub>d</sub>	S <sub>d</sub>	C <sub>d</sub>	H <sub>d</sub>	N <sub>d</sub>	O <sub>d</sub>	Cl <sub>d</sub>	
<b>American</b>											
PRB	27.70	8.00	48.30	42.90	0.57	67.30	4.58	0.96	19.92	0.01	28.04
IL#6	13.50	10.00	42.00	48.00	3.47	71.00	5.00	1.30	9.13	0.11	29.60
<b>Chinese</b>											
S01	8.41	44.64	23.64	31.72	1.47	38.88	2.35	0.64	12.02	0.01	13.54
S04	3.80	22.97	10.54	66.49	2.79	67.03	2.55	1.00	3.66	0.03	25.98
S07	9.14	24.82	27.80	47.38	0.53	57.69	3.46	0.90	12.60	0.36	21.87
S10	15.71	5.68	34.39	59.93	0.45	74.54	4.39	0.94	14.00	0.01	28.48
M = Moisture, VM = Volatile Matter, FC - Fixed Carbon											
<sup>ad</sup> air-dried <sup>d</sup> dry, * as-received											

## 5.2 Coal Sample Characterization

To prepare each coal sample for combustion in the drop-tube furnace, as-received samples were air-dried in a desiccating chamber, ground with a household electric

grinder, and separated into the 150-mesh size (100  $\mu\text{m}$ ) fraction with a standard 8" sieve and a mechanical vibrator. In the absence of information on the mineral content of the selected Chinese coal samples, x-ray diffraction (XRD) was used to identify the major mineral constituents of sample. Figure 5.1 is a stacked plot of XRD spectra for respective coal samples, with labeled peaks denoting the presence of matching mineral compounds. The matched mineral phases for each sample are listed as follows:

- PRB: quartz ( $\text{SiO}_2$ ), kaolinite ( $\text{Al}_2\text{Si}_2\text{O}_5(\text{OH})_4$ )
- Illinois #6: quartz ( $\text{SiO}_2$ ), pyrite ( $\text{FeS}_2$ ), kaolinite ( $\text{Al}_2\text{Si}_2\text{O}_5(\text{OH})_4$ )
- S01-Lignite: kaolinite ( $\text{Al}_2\text{Si}_2\text{O}_5(\text{OH})_4$ ), quartz ( $\text{SiO}_2$ )
- S04-Anthracite: kaolinite ( $\text{Al}_2\text{Si}_2\text{O}_5(\text{OH})_4$ ), pyrite ( $\text{FeS}_2$ ), quartz ( $\text{SiO}_2$ ), calcite ( $\text{CaCO}_3$ )
- S07-Subbituminous: kaolinite ( $\text{Al}_2\text{Si}_2\text{O}_5(\text{OH})_4$ ), boehmite ( $\text{AlO}(\text{OH})$ ), pyrite ( $\text{FeS}_2$ ), siderite ( $\text{FeCO}_3$ ), calcite ( $\text{CaCO}_3$ ), hematite ( $\text{Fe}_2\text{O}_3$ )
- S10-Bituminous: quartz ( $\text{SiO}_2$ ), kaolinite ( $\text{Al}_2\text{Si}_2\text{O}_5(\text{OH})_4$ )

Kaolinite transforms into a variety of species, depending on temperature, coal composition, and local combustion conditions (oxidizing or reducing). Between 1300 K and 1500 K, kaolinite simply fuses and remains as aluminosilicate fly ash. Above 1500 K, for bituminous coals, kaolinite transforms to mullite ( $3\text{Al}_2\text{O}_3\text{-}2\text{SiO}_2$ ) and aluminum oxide ( $\text{Al}_2\text{O}_3$ ), while for lignites, it may interact with CaO to form gehlenite ( $2\text{CaO-SiO}_2\text{-Al}_2\text{O}_3$ ) or anorthite ( $\text{CaO-}2\text{SiO}_2\text{-Al}_2\text{O}_3$ ).<sup>63</sup>

Pyrite rapidly forms iron sulfide (FeS) at high temperature (~1473 K). This subsequently becomes iron (III) oxide (Fe<sub>2</sub>O<sub>3</sub>) under oxidizing conditions, possibly forming Fe<sub>3</sub>O<sub>4</sub> under reducing conditions before being oxidized to Fe<sub>2</sub>O<sub>3</sub>. Calcite also undergoes rapid transformation into CaO at high temperatures (1273-1830 K), and CaO may remain isolated in fly ash or become associated with the aluminosilicate transformations of kaolinite.<sup>33</sup> These findings are useful for correlating mineral content of collected submicrometer fly ash particles with known or postulated aspects of the coal combustion process, such as comparing calculated values of vaporized metal-oxides to measured amounts of submicrometer particles.

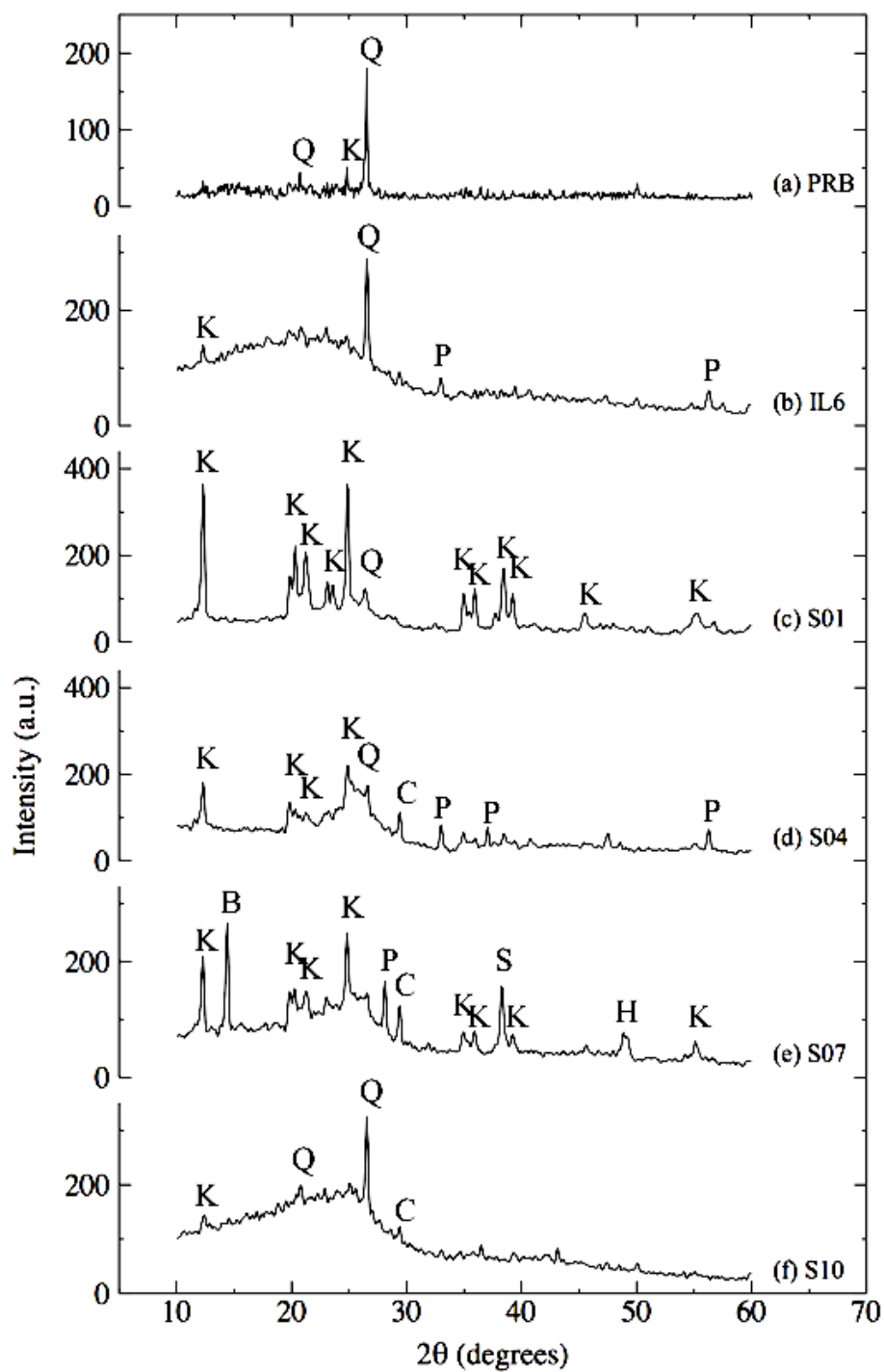
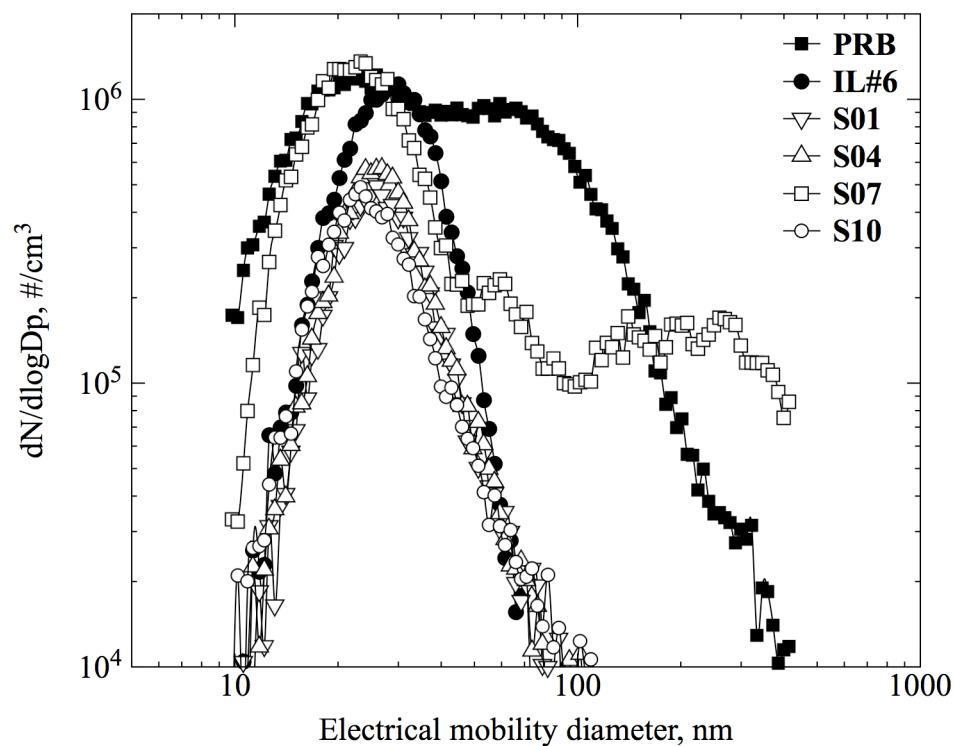


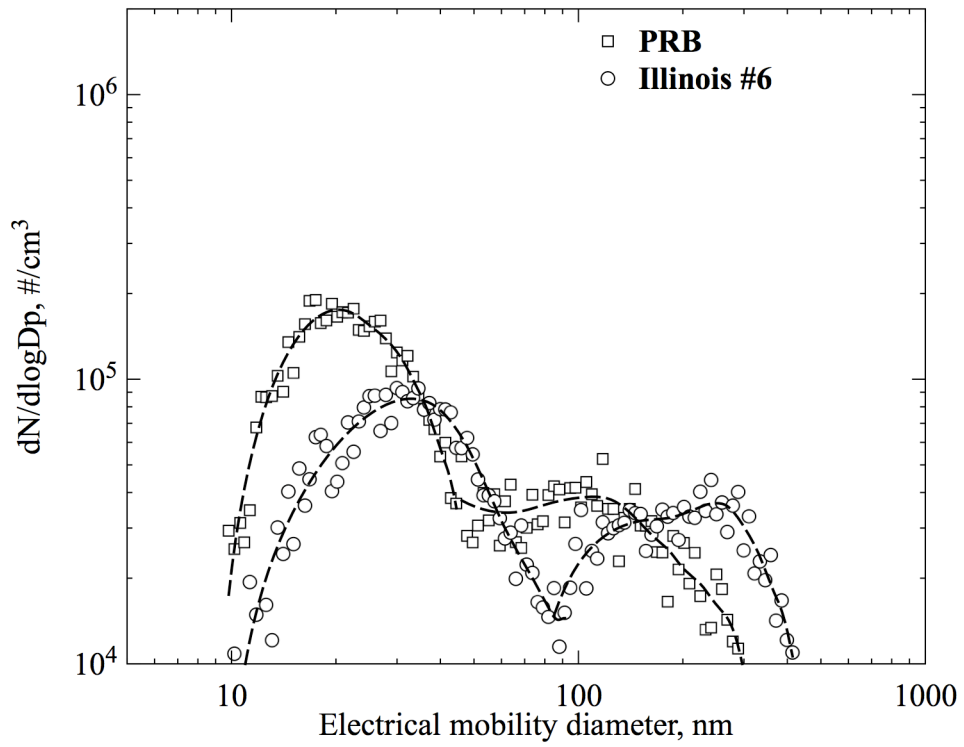
Figure 5.1 X-Ray Diffraction Spectra for Selected American & Chinese Coals (Q-Quartz, K-Kaolinitie, P-Pyrite, C-Calcite, B-Boehmite, S-Siderite, H-Hematite)

## 5.3 Results and Discussion

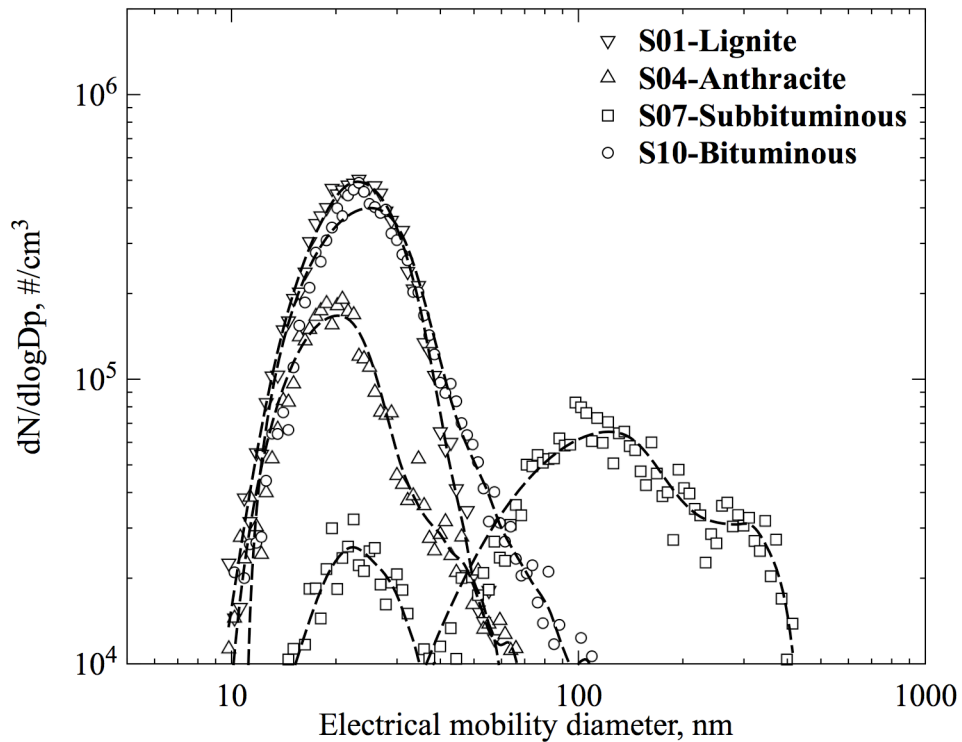
Samples of each of the selected coals were combusted in air, and their respective submicrometer particle size distributions are shown in Figure 5.2. The same samples were then combusted in O<sub>2</sub>-CO<sub>2</sub> (oxy-combustion) at a fixed flue-gas recycle ratio (40%), and the particle size distributions for the American and Chinese coals in this case are shown Figures 5.3 and 5.4 respectively.



**Figure 5.2 Submicrometer Particle Size Distributions for Conventional Coal-Air Combustion with American & Chinese Coals at a Fixed O<sub>2</sub>/Coal Molar Ratios (~12.6)**



**Figure 5.3 Submicrometer Particle Size Distributions for Oxy-Coal Combustion with American Coals at a Fixed Flue-Gas Recycle Ratio (40%)**



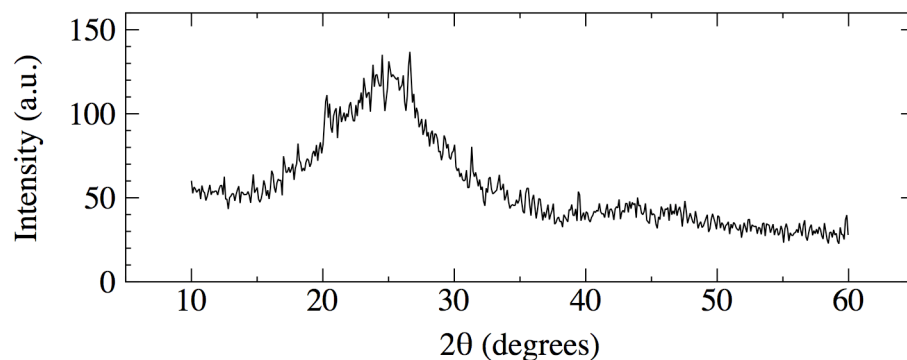
**Figure 5.4 Submicrometer Particle Size Distributions for Oxy-Coal Combustion with Chinese Coals at a Fixed Flue-Gas Recycle Ratio (40%)**

Table 5.3 contains the summary statistics for the particle size distributions of all the combustion conditions involving varied coal types. In air, the subbituminous PRB and S07 coals were found to generate the highest number concentration of submicrometer particles, while the lignite, S01, generated the lowest number concentration of submicrometer particles, presumably due to it having the lowest calorific value of all the samples tested.

**Table 5.3 Summary Statistics for Submicrometer Particle Size Distributions during Combustion of American & Chinese Coals during Conventional-Air and Oxy-Combustion Conditions**

Set	#	System	Coal Name	Coal Rank	$N_{total}$ (#/cm <sup>3</sup> )	$d_{pg}$ (nm)	$\sigma_g$	$A_{total}$ (nm <sup>2</sup> /cm <sup>3</sup> )	$V_{total}$ (nm <sup>3</sup> /cm <sup>3</sup> )
IV	1	Coal- O <sub>2</sub> /N <sub>2</sub>	PRB	Subbituminous	$9.49 \times 10^5$	37.7	2.0	$1.22 \times 10^{10}$	$2.73 \times 10^{11}$
	2		IL#6	Bituminous	$3.46 \times 10^5$	28.2	1.4	$1.70 \times 10^8$	$2.16 \times 10^9$
	3		S01	Lignite	$1.48 \times 10^5$	27.5	1.4	$4.95 \times 10^8$	$4.23 \times 10^9$
	4		S04	Anthracite	$1.68 \times 10^5$	27.2	1.4	$4.73 \times 10^8$	$5.48 \times 10^9$
	5		S07	Subbituminous	$6.05 \times 10^5$	33.7	2.3	$1.60 \times 10^{10}$	$6.84 \times 10^{11}$
	6		S10	Bituminous	$1.51 \times 10^5$	25.7	1.5	$5.27 \times 10^8$	$6.84 \times 10^9$
	7	Coal- O <sub>2</sub> /CO <sub>2</sub>	PRB	Subbituminous	$1.00 \times 10^5$	32.3	2.3	$1.86 \times 10^9$	$6.35 \times 10^{10}$
	8		IL#6	Bituminous	$2.05 \times 10^5$	89.4	1.6	$7.73 \times 10^9$	$1.99 \times 10^{11}$
	9		S01	Lignite	$1.64 \times 10^5$	23.1	1.4	$3.90 \times 10^8$	$4.09 \times 10^9$
	10		S04	Anthracite	$5.81 \times 10^4$	21.8	1.5	$1.61 \times 10^8$	$2.40 \times 10^9$
	11		S07	Subbituminous	$4.81 \times 10^4$	95.6	2.3	$3.75 \times 10^9$	$1.54 \times 10^{11}$
	12		S10	Bituminous	$1.26 \times 10^5$	22.2	1.5	$3.55 \times 10^8$	$6.02 \times 10^9$
Total flow rate = 3 lpm, coal feed rate = 2 g/hr, O <sub>2</sub> /coal ratio = 6.36									
Furnace temperature = 1100 °C									

The bituminous S07 was observed to be bimodal, with one mode ~25 nm and another ~120 nm when combusted in air and similarly when combusted in the O<sub>2</sub>-CO<sub>2</sub> mode. Second modes also appeared between 100 nm and 300 nm for PRB and Illinois #6 coals during oxy-combustion. This second mode was possibly populated by soot particles as reported by Fletcher *et al.*<sup>49</sup>. Figure 5.5 is the x-ray diffractogram of a submicrometer sample collected during oxy-combustion of Illinois #6.



**Figure 5.5 X-Ray Diffractogram of Submicrometer Particles Collected during Combustion of Illinois #6 Coal in Air**

The diffractogram confirms that the sample was largely non-crystalline and consistent with possible coal-derived soot. The submicrometer particles were also collected during combustion of S07 in air and were examined using an SEM. Figure 5.6 is an electron micrograph of this sample, showing spherical submicrometer particles and well-sintered agglomerates, but no indication of soot agglomerates. Figures 5.3 and 5.4 suggest that the incidence of soot formation may be promoted by replacing conventional (air) combustion with oxy-coal combustion, creating a more pervasive reducing environment in which soot yield may either be enhanced or post-combustion soot oxidation may be suppressed. However, the emergence of a second mode ~100 nm may also be due to metal-oxide particle growth by coagulation, since it has recently been reported by Zhang *et al.* through direct high-speed camera observations that buoyancy forces due to the evolution of tar volatile matter from bituminous coal can significantly retard the particle motion in a drop-tube furnace,

particularly in the early stages of combustion<sup>64</sup>. This may lead to longer than predicted time available for coagulation and sintering, and at higher temperatures.

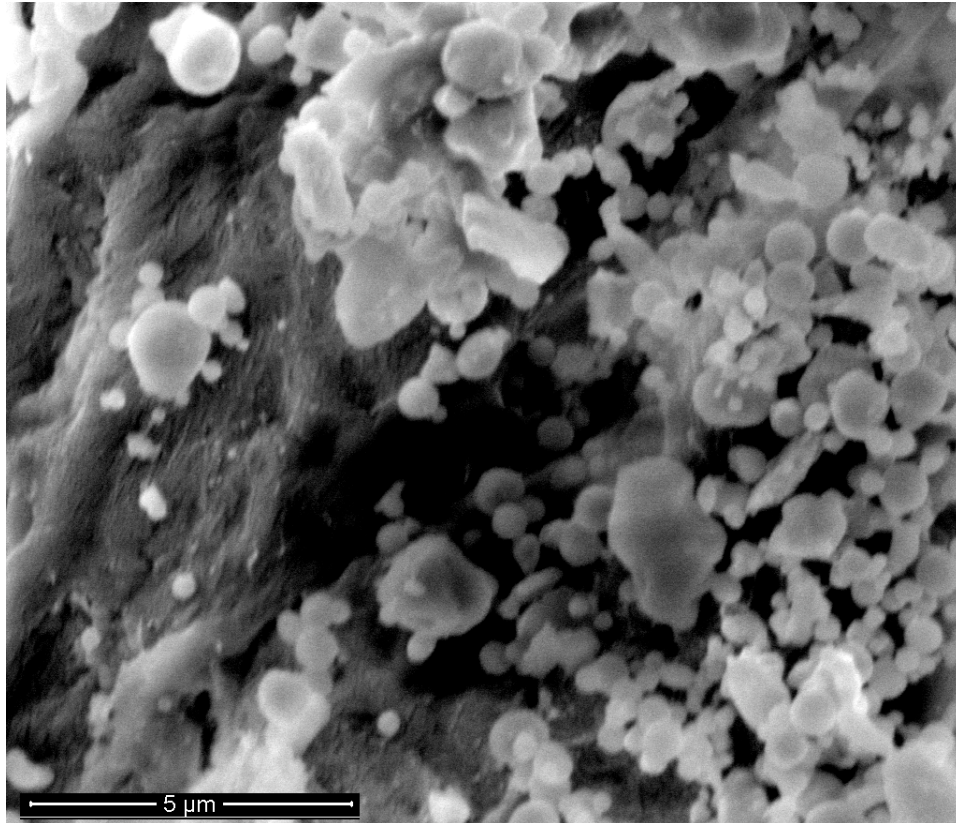


**Figure 5.6 Scanning Electron Micrograph of Total Ash Particles Collected during Oxy-Combustion of S07 Coal**

For all samples (excepting the lignite S01), switching from air to O<sub>2</sub>-CO<sub>2</sub> resulted in a reduction in the total number concentration, and for PRB, Illinois #6, and S07, the persistence of a mode ~100-300 nm. However, there is no apparent relationship between the presence of this mode and the coal rank, since a similar mode was not

observed during the combustion of the bituminous S10 coal, which is most similar to the bituminous Illinois #6 sample.

Considering the summary statistics of the submicrometer particle size distributions in Table 5.3, two pairs of correlations were extracted: one for the coal-air cases and one for the oxy-coal with recycle case. The first correlation in each pair consists of the total number concentration and the fixed carbon content for each coal, while the second consists of the geometric mean diameter and the fixed carbon content for each coal. With the exception of Chinese lignite, which had the lowest heating value, significant negative correlations between fixed carbon content and both total number concentration and geometric mean diameter were observed for coal-air combustion. In other words, higher fixed carbon content corresponded to lower mean diameters and lower total number concentrations. Recall that the higher the fixed carbon content, the lower the sum of volatile matter and ash content (on a dry basis). Figures 5.7 and 5.8 are scatter plots of total number concentration and geometric mean diameter respectively, each plotted against fixed carbon content for respective coal samples.

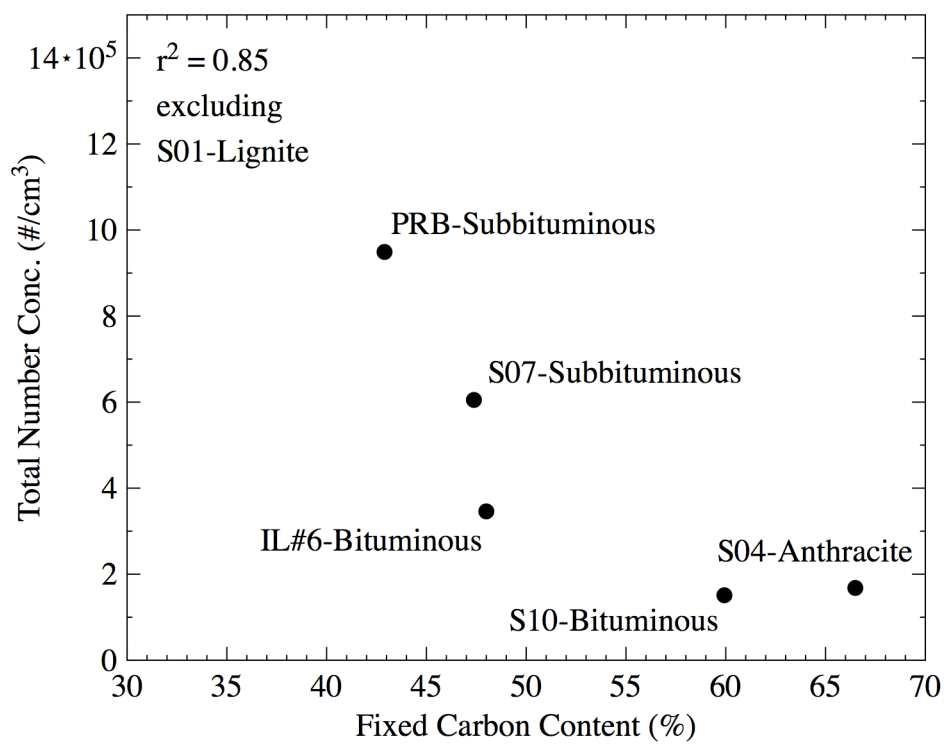


**Figure 5.7 Scatter Plot of Total Number Concentration vs. Fixed Carbon Content for Submicrometer Particles Sampled during Coal-Air Combustion**

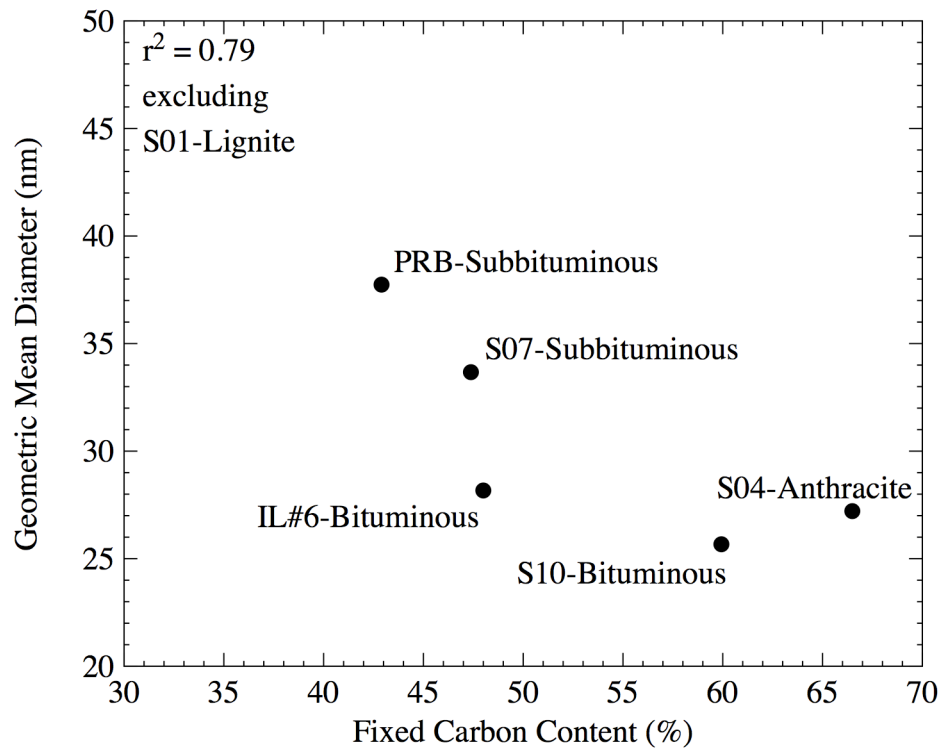


**Figure 5.8 Scatter Plot of Geometric Mean Diameter vs. Fixed Carbon Content for Submicrometer Particles Sampled during Coal-Air Combustion**

For the coal-air cases, the negative correlations between fixed carbon content and total number concentration and geometric mean diameter were strong ( $r^2=0.85$  and  $0.79$  respectively), while for the oxy-coal cases (shown in Figures 5.9 and 5.10), the corresponding correlations were insignificant ( $r^2=0.25$  and  $0.58$  respectively). The absence of significant correlations during oxy-coal combustion may be attributed to the demonstrated suppressive effect of  $\text{CO}_2$  on metal-oxide vaporization and the disparate degrees of suppression due to the varied mineral composition of the coals used.

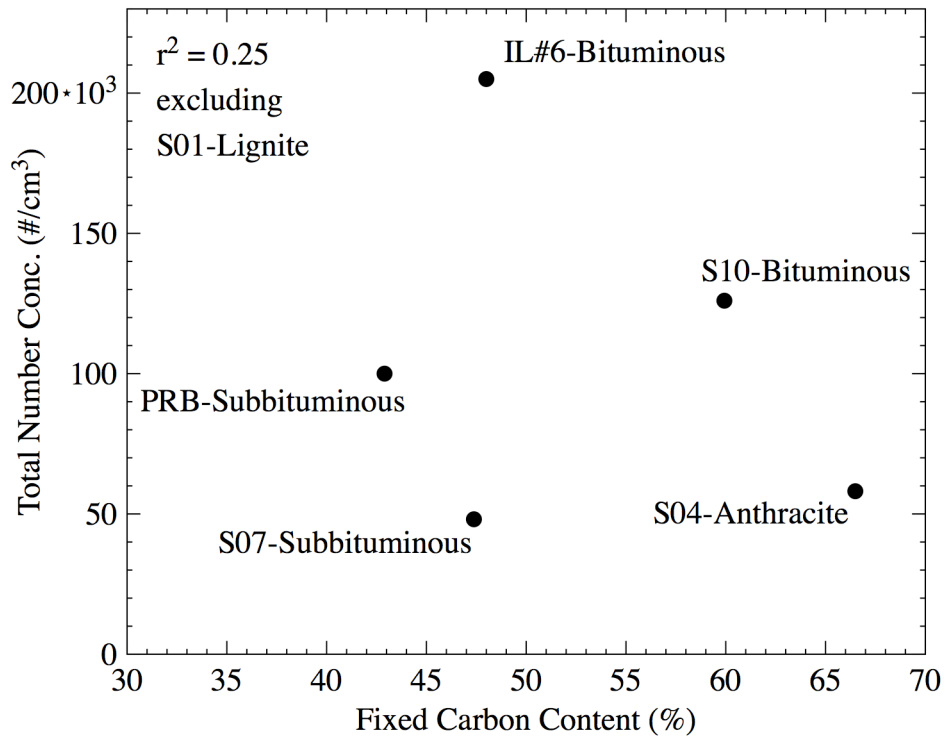


**Figure 5.9 Scatter Plot of Total Number Concentration vs. Fixed Carbon Content for Submicrometer Particles Sampled during Oxy-Coal Combustion with 40% Flue-Gas Recycle Ratio**

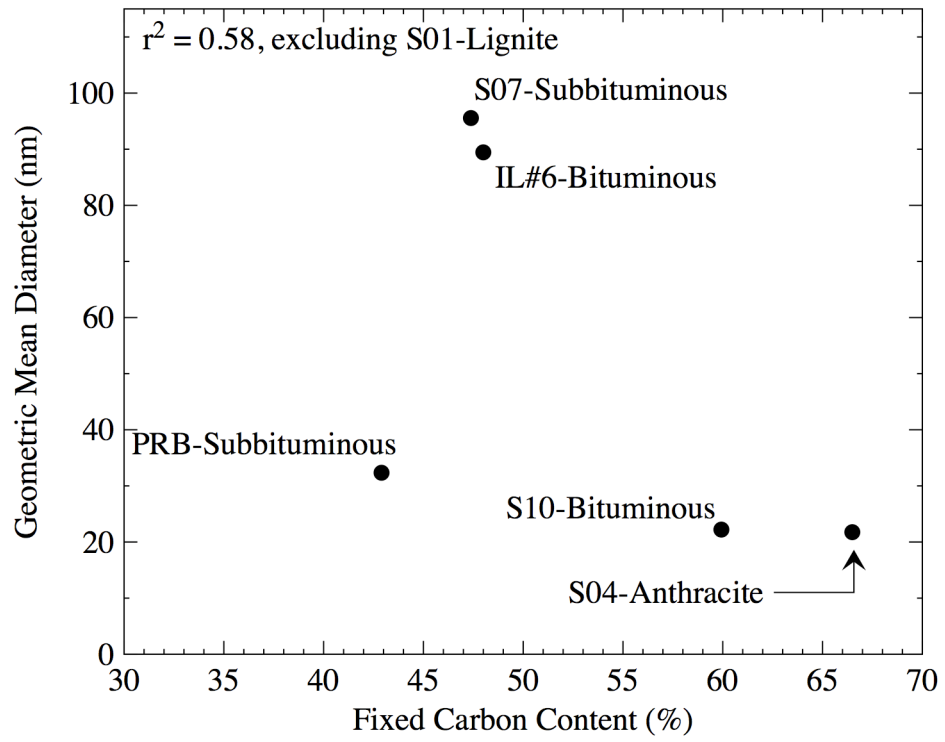


**Figure 5.10 Scatter Plot of Geometric Mean Diameter vs. Fixed Carbon Content for Submicrometer Particles Sampled during Oxy-Coal Combustion with 40% Flue-Gas Recycle Ratio**

# Chapter 6

## Summary & Conclusions

The role of flue-gas recycle in submicrometer particle formation was investigated in three steps: (1) understanding the effect of gas composition on the metal-oxide vaporization and chemical nucleation pathway by varying the  $O_2$ /coal ratio during combustion of Powder River Basin (PRB) coal in two distinct systems—the conventional  $O_2$ - $N_2$  system and the oxy-coal  $O_2$ - $CO_2$  system; (2) characterizing the effect of flue-gas recycle on  $CO_2$  concentration at the furnace inlet to better estimate the  $O_2$ /coal ratio during oxy-combustion experiments with flue-gas recycle; and (3) assessing submicrometer particle formation during oxy-combustion with flue-gas recycle by combusting two American and four Chinese coals, spanning the range of ASTM coal ranks.

Gas compositions, particularly bulk concentrations of  $O_2$  and  $CO_2$ , play a key role in determining both the adiabatic flame temperature as well as actual char surface temperatures during burnout. And, the char surface temperature and the temperature in the vicinity of the burning char particle is a critical parameter in multiple metal-

oxide/sub-oxide vaporization equilibria, with the O<sub>2</sub>-CO<sub>2</sub> system more sensitive to the vaporization temperature than the O<sub>2</sub>-N<sub>2</sub> system.

The flue-gas recycle ratio was introduced as the ratio of the flue-gas volume flow rate to the total volume flow rate through the furnace, such that steady flue-gas recycling was achieved for ratios up to 80%. Particle size distribution measurements of PRB fly ash during oxy-combustion with flue-gas recycle did not show significant change with increasing flue-gas recycle ratio. Increasing flue-gas recycle from no-recycle to 80% recycle was found to slightly reduce the O<sub>2</sub>/coal molar ratio from 12.6 to 12.3, and a corresponding decrease of 4 nm in the geometric mean size of the submicrometer particle size distribution was observed by differential mobility analysis. This implies that previous results from experiments performed with once-through laboratory-scale systems retain their applicability with respect to mechanisms of submicrometer particle formation.

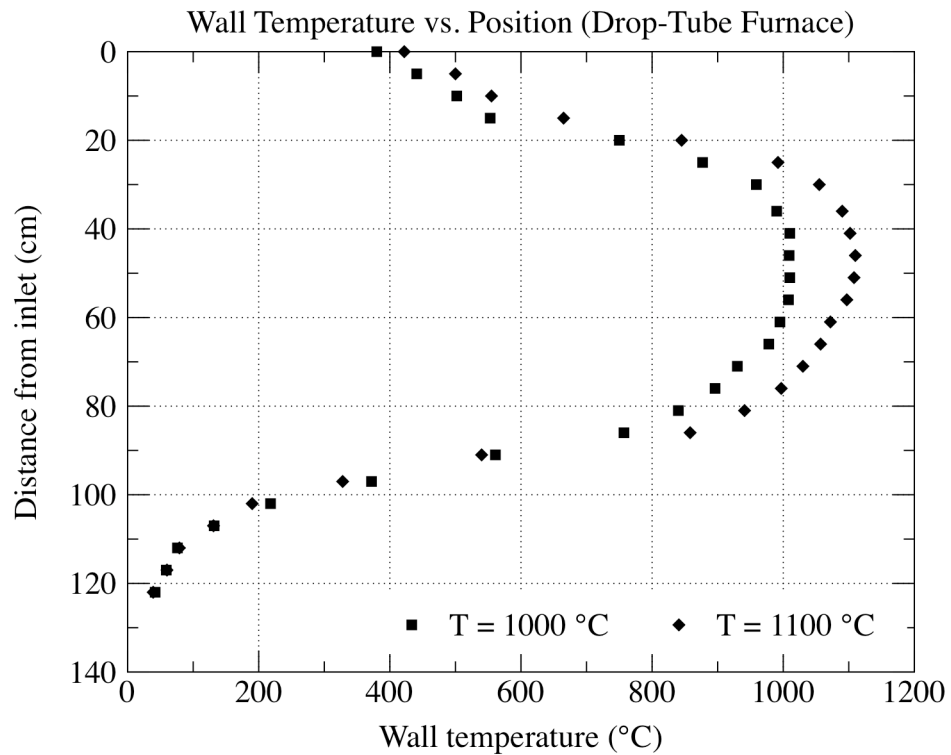
Two American coals (subbituminous PRB and bituminous Illinois #6) were used in conjunction with four Chinese coal samples, each of different ASTM rank (S01-lignite, S04-anthracite, S07-subbituminous, and S10-bituminous). In consonance with reported results in the literature, Illinois #6 was found to yield submicrometer particles believed to be soot agglomerates (~100-200 nm) in addition to fly ash (~25 nm) during oxy-combustion with flue-gas recycle, likely due to the modest furnace wall temperature (1373 K) compared with other combustion studies and locally

reducing conditions more favorable to coal devolatilization and gas-phase soot formation reactions than soot oxidation. Larger-than-estimated coal particle residence times, particularly in the early stages of burnout at the highest-temperature regions of the furnace, may also contribute to the emergence of additional, larger modes among bituminous coals with high volatile matter content. Excepting the low-heating-value Chinese lignite sample (S01), both American and Chinese coals were found to exhibit negative correlations between their fixed carbon content and the total number concentration and geometric mean diameter of submicrometer particles. These correlations were found to be stronger for coal-air combustion than during oxy-coal combustion with flue-gas recycle, likely due to the suppressive effect of CO<sub>2</sub> on metal-oxide vaporization during oxy-coal combustion. Scanning electron microscopy was also used to verify that the vaporization-nucleation-pathway was dominant in for the submicrometer particles measured, and the suppressive effect of CO<sub>2</sub> on the vaporization pathway was confirmed by noting that the total number concentrations of submicrometer particles were lower during oxy-combustion with recycle compared to combustion in air for all coals, except the Chinese lignite S01, whose total number concentration of submicrometer particles did not undergo significant change.

# Appendix A

## Drop-Tube Furnace Temperature Profiles

The furnace temperature profiles measured for two furnace temperature set-points are shown below (from Smallwood<sup>51</sup>):



# Appendix B

## Flow Parameter Calculations for Drop-Tube Furnace Setup

Using the dimensions of the alumina furnace reactor tube (2.5-in. ID, 48-in. length), as well as the furnace temperature profile, process flow parameters such as the residence time were calculated as follows:

### Residence Time

The gas residence time in the furnace was estimated in three sections of the tube length, from the top of the tube (section 1: 0-10 in., section 2: 10-32 in., section 3: 32-48 in.). Average temperatures for each of these sections were then used for each section, based on the temperature profile of Appendix A.

Applying the ideal gas law, we find that the product of the gas density and temperature are constant.

$$\rho T = PM/R = 352.8 \text{ K kg/m}^3$$

where  $\rho$  is the gas density,  $T$  is the average temperature in a section,  $P$  is the pressure,  $M$  is the molar mass of gas, and  $R$  is the ideal gas constant. Based on mass conservation and an inlet gas flow rate  $Q_0$ , the mass flow rate  $\rho_0 Q_0$  into the furnace is also constant, and the residence time for the entire tube length can be calculated as follows:

$$t_{res} = \frac{\pi r^2 L_1}{Q_1} + \frac{\pi r^2 L_2}{Q_2} + \frac{\pi r^2 L_3}{Q_3}$$

where  $r$  is the inner radius of the alumina tube

## Gas Temperature

The gas temperature for each section of the furnace tube was estimated using correlations for forced convection heat transfer in a fully-developed laminar flow pipe (Incopera and DeWitt, *Fundamentals of Heat and Mass Transfer*, 5<sup>th</sup> ed., 2002).

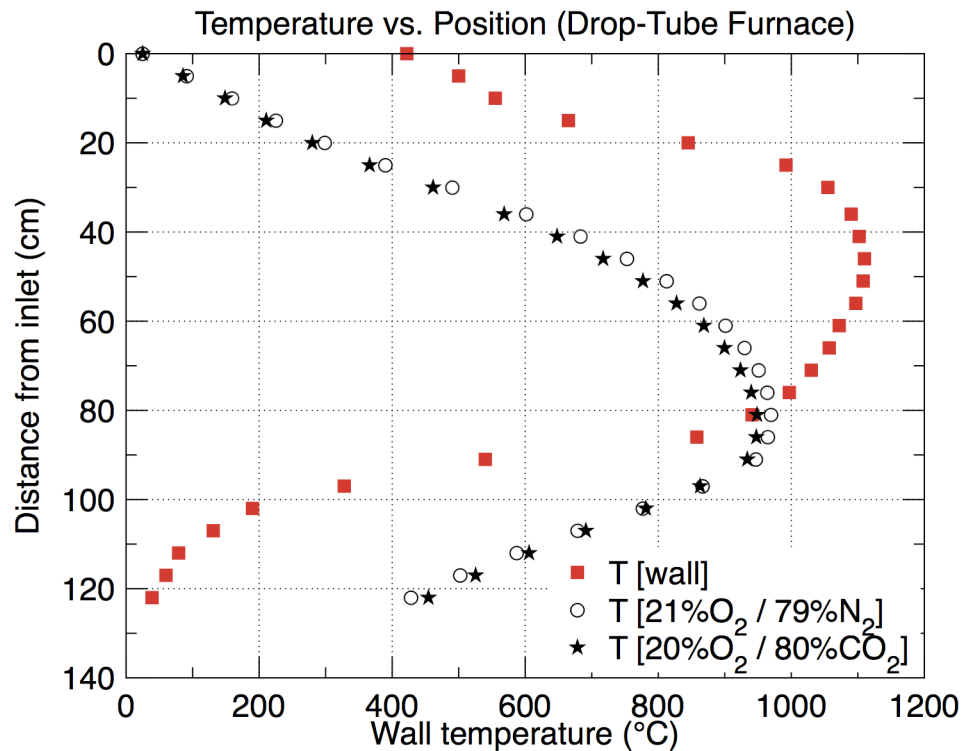
$$T_{gas,i} = T_{wall} - (T_{wall} - T_{gas,i-1}) \cdot \exp\left(-\frac{\pi DL_i h}{m C_p}\right)$$

where

$$h = \frac{Nu \cdot k_{gas}}{D}$$

and  $h$  is the convective heat transfer coefficient,  $D$  is the inner diameter of the alumina tube,  $L_i$  is the length of the tube section,  $C_p$  is the specific heat capacity of the gas,  $Nu$  is the Nusselt number ( $=3.66$  for uniform tube wall temperature), and  $k_{gas}$  is the thermal conductivity of the gas.

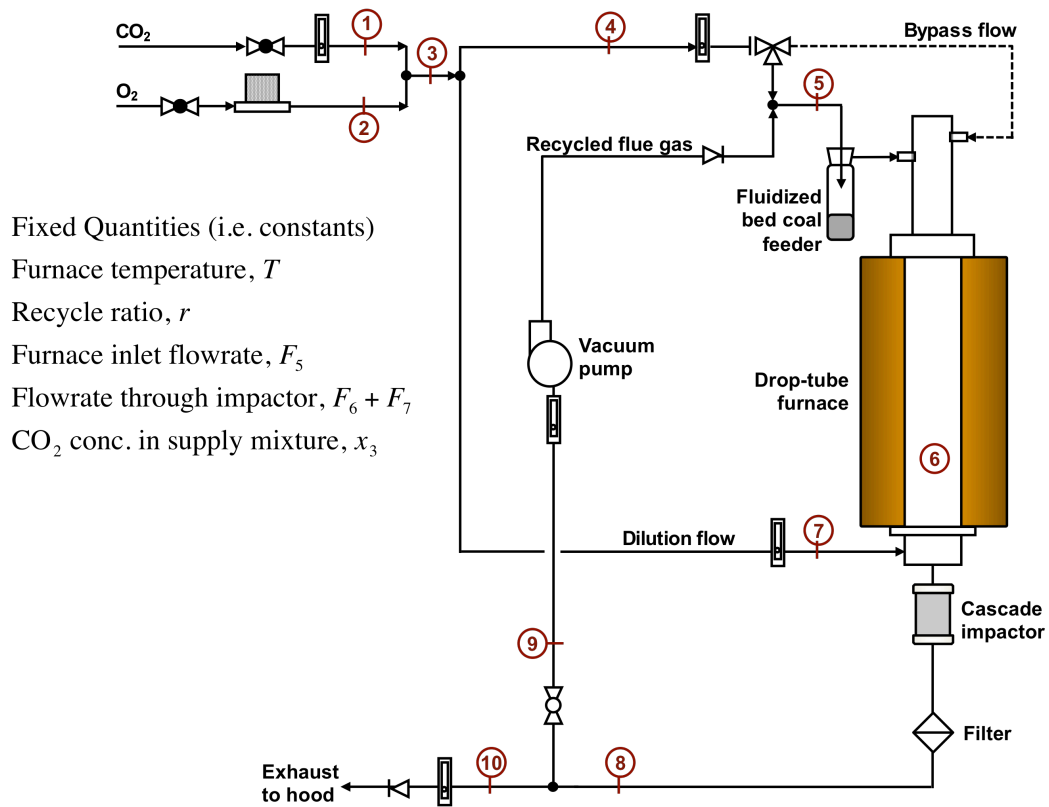
A plot of the calculated gas temperature, as outlined above, for air and an O<sub>2</sub>-CO<sub>2</sub> mixture (20%-80%) is as follows, with the measured temperature profile (from Smallwood<sup>51</sup>) of the furnace wall overlaid.



# Appendix C

## System Mole Balances for CO<sub>2</sub>

Mole balances were applied on a node-by-node basis as follows:



Fixed Quantities (i.e. constants)

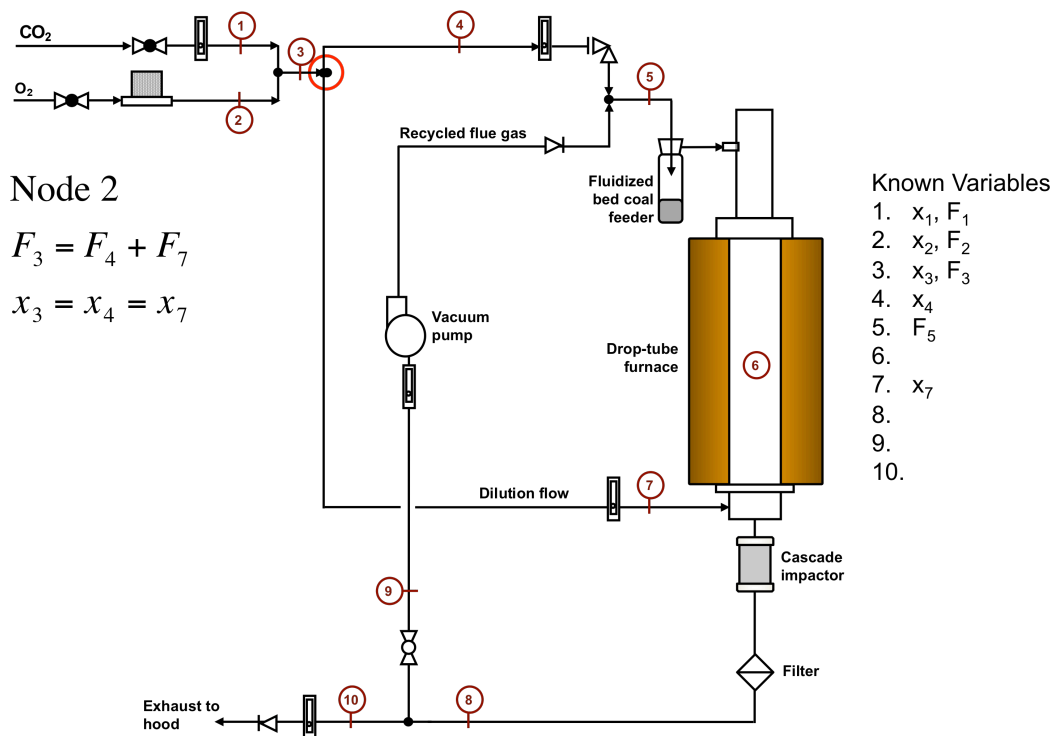
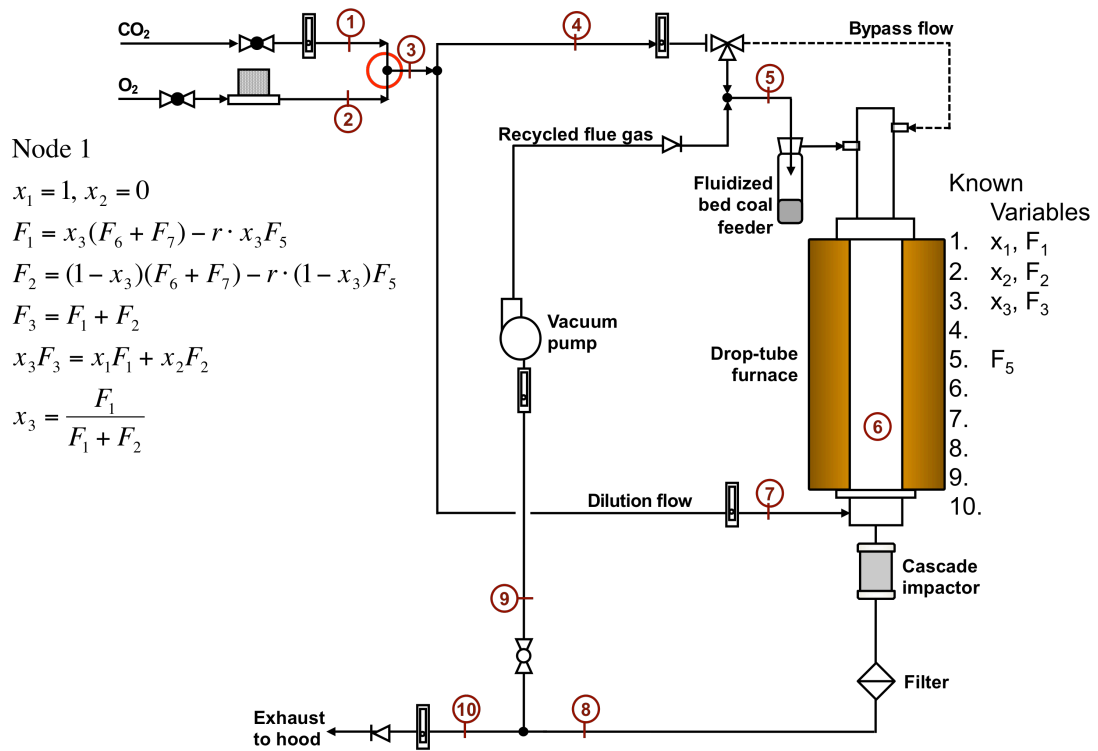
Furnace temperature,  $T$

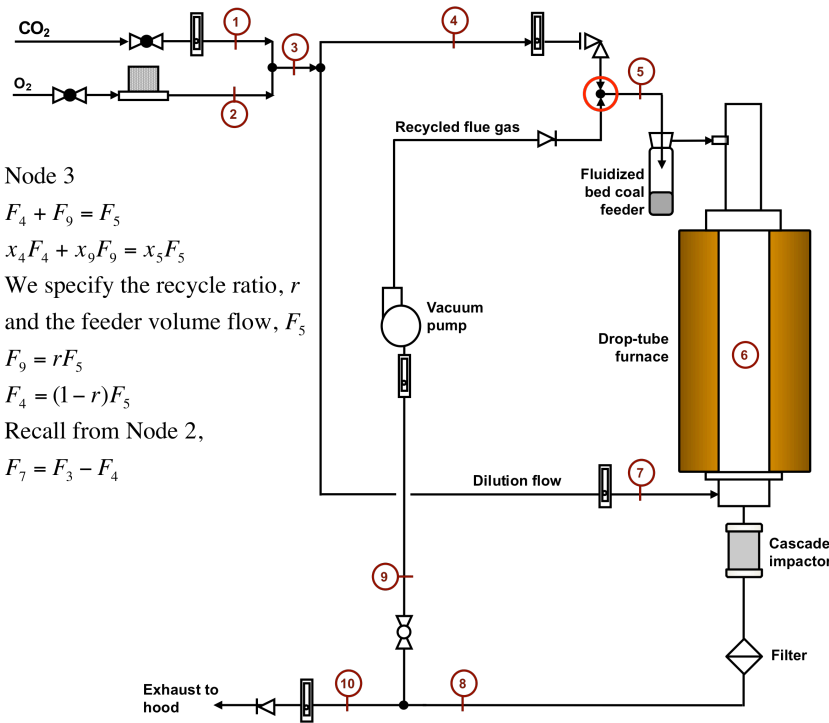
Recycle ratio,  $r$

Furnace inlet flowrate,  $F_5$

Flowrate through impactor,  $F_6 + F_7$

CO<sub>2</sub> conc. in supply mixture,  $x_3$





Node 3

$$F_4 + F_9 = F_5$$

$$x_4 F_4 + x_9 F_9 = x_5 F_5$$

We specify the recycle ratio,  $r$   
and the feeder volume flow,  $F_5$

$$F_9 = r F_5$$

$$F_4 = (1 - r) F_5$$

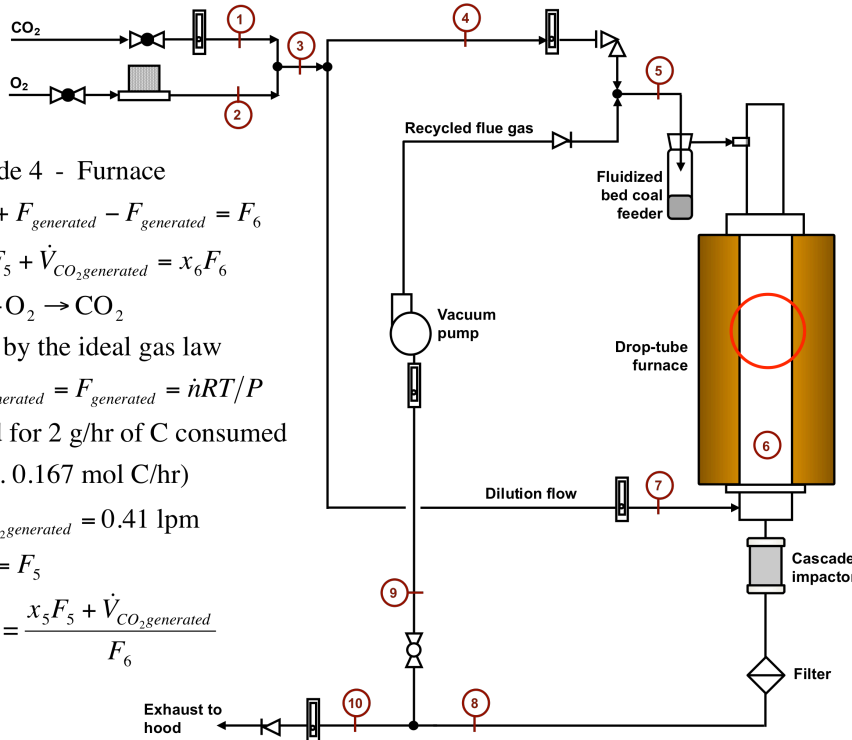
Recall from Node 2,

$$F_7 = F_3 - F_4$$

Known Variables

1.  $x_1, F_1$
2.  $x_2, F_2$
3.  $x_3, F_3$
4.  $x_4, F_4$
5.  $F_5$
- 6.
7.  $x_7, F_7$
- 8.
9.  $F_9$
- 10.

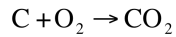
Recycle ratio,  $r$



Node 4 - Furnace

$$F_5 + F_{generated} - F_{generated} = F_6$$

$$x_5 F_5 + \dot{V}_{CO_2, generated} = x_6 F_6$$



so, by the ideal gas law

$$F_{generated} = \dot{V}_{generated} = \dot{n}RT/P$$

and for 2 g/hr of C consumed

(i.e. 0.167 mol C/hr)

$$\dot{V}_{CO_2, generated} = 0.41 \text{ lpm}$$

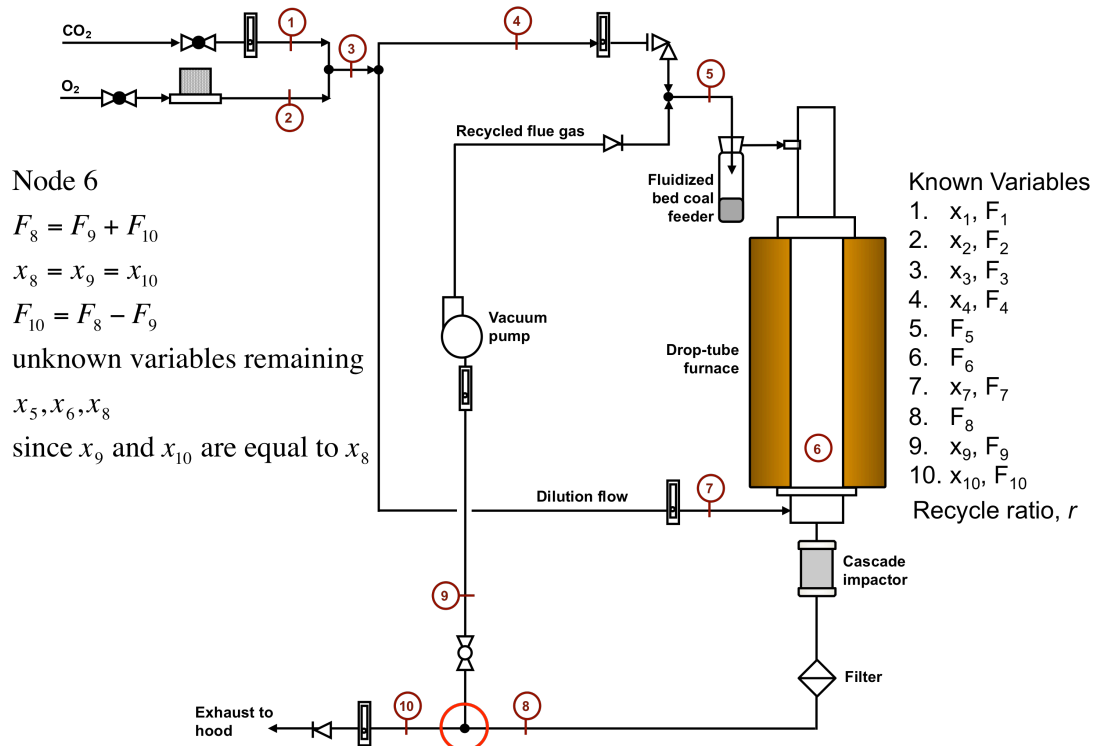
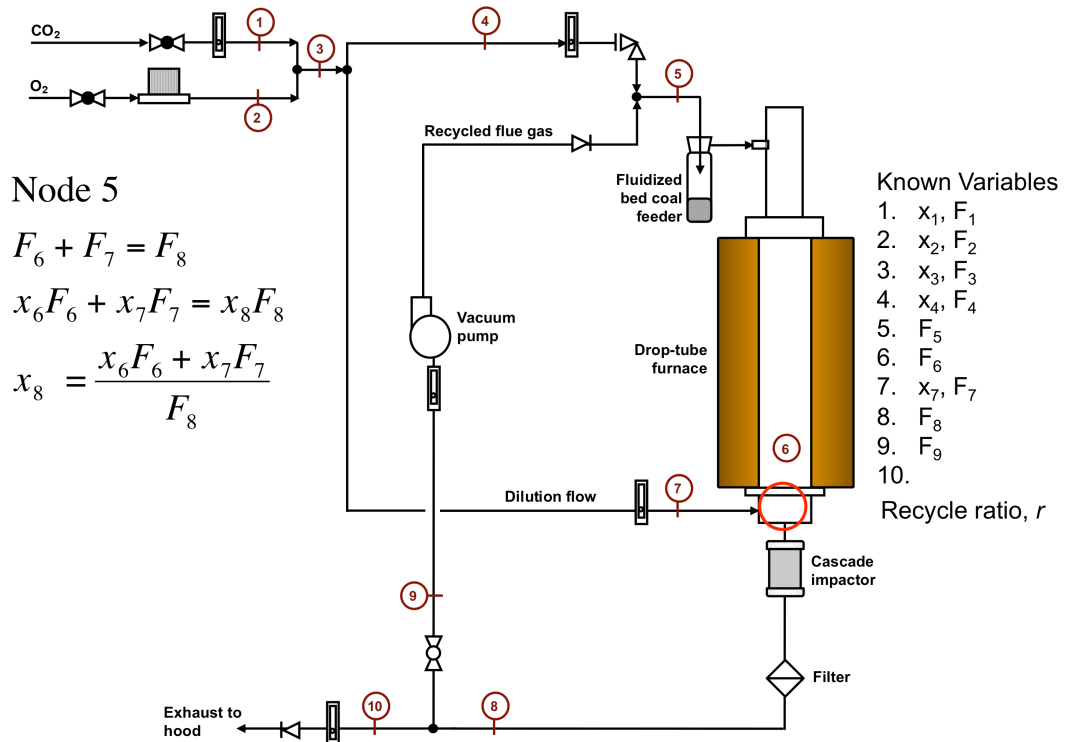
$$F_6 = F_5$$

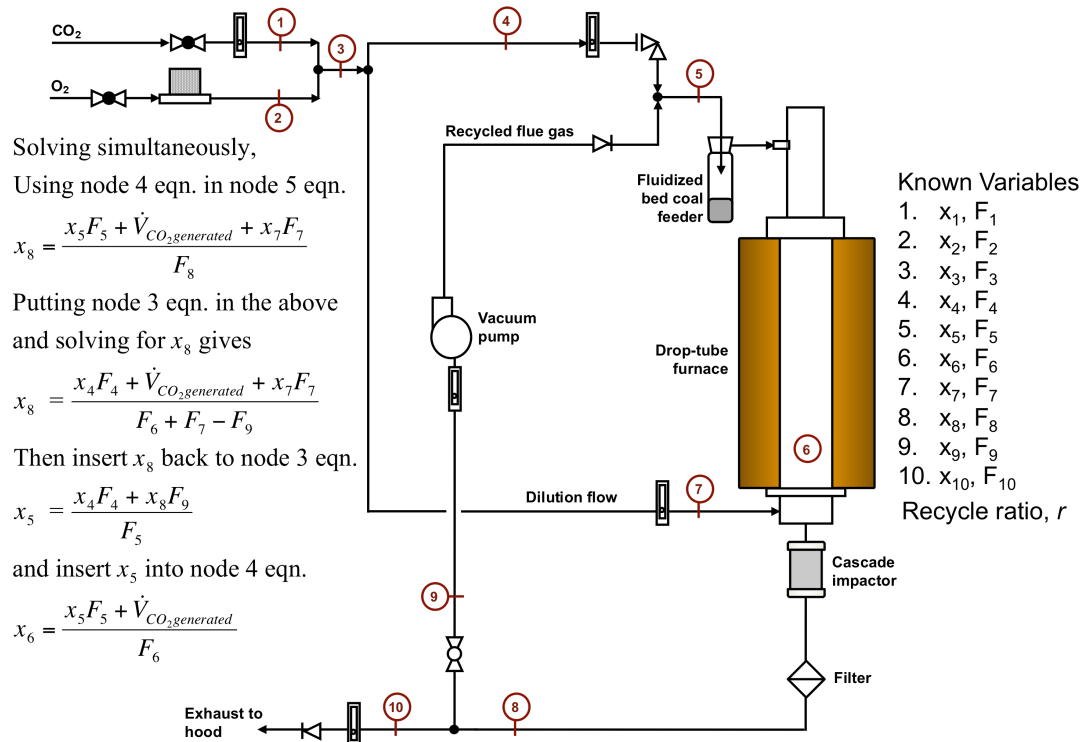
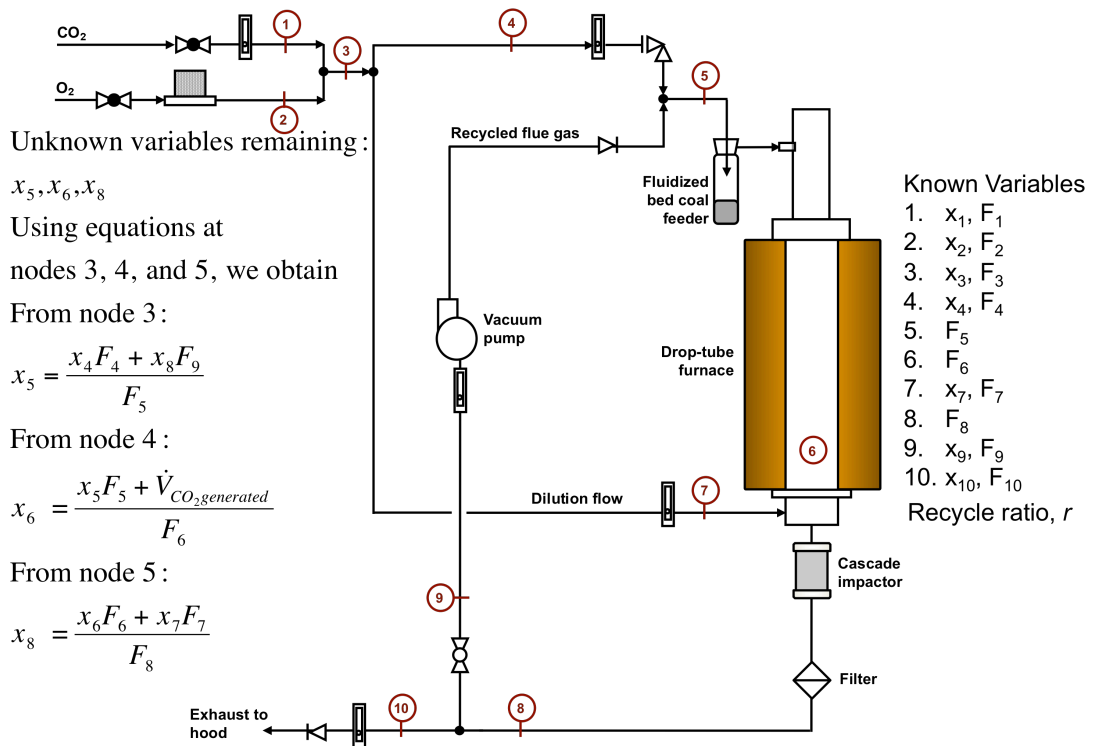
$$x_6 = \frac{x_5 F_5 + \dot{V}_{CO_2, generated}}{F_6}$$

Known Variables

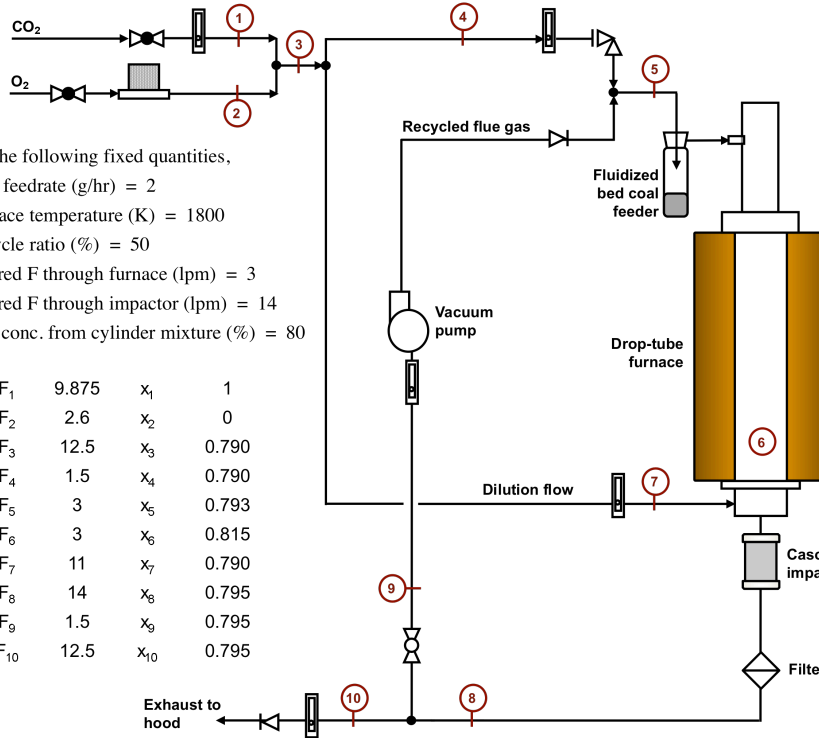
1.  $x_1, F_1$
2.  $x_2, F_2$
3.  $x_3, F_3$
4.  $x_4, F_4$
5.  $F_5$
6.  $F_6$
7.  $x_7, F_7$
- 8.
9.  $F_9$
- 10.

Recycle ratio,  $r$





### Example Calculation



For the following fixed quantities,

Coal feedrate (g/hr) = 2

Furnace temperature (K) = 1800

Recycle ratio (%) = 50

Desired F through furnace (lpm) = 3

Desired F through impactor (lpm) = 14

CO<sub>2</sub> conc. from cylinder mixture (%) = 80

F <sub>1</sub>	9.875	x <sub>1</sub>	1
F <sub>2</sub>	2.6	x <sub>2</sub>	0
F <sub>3</sub>	12.5	x <sub>3</sub>	0.790
F <sub>4</sub>	1.5	x <sub>4</sub>	0.790
F <sub>5</sub>	3	x <sub>5</sub>	0.793
F <sub>6</sub>	3	x <sub>6</sub>	0.815
F <sub>7</sub>	11	x <sub>7</sub>	0.790
F <sub>8</sub>	14	x <sub>8</sub>	0.795
F <sub>9</sub>	1.5	x <sub>9</sub>	0.795
F <sub>10</sub>	12.5	x <sub>10</sub>	0.795

### Known Variables

1. x<sub>1</sub>, F<sub>1</sub>
2. x<sub>2</sub>, F<sub>2</sub>
3. x<sub>3</sub>, F<sub>3</sub>
4. x<sub>4</sub>, F<sub>4</sub>
5. x<sub>5</sub>, F<sub>5</sub>
6. x<sub>6</sub>, F<sub>6</sub>
7. x<sub>7</sub>, F<sub>7</sub>
8. x<sub>8</sub>, F<sub>8</sub>
9. x<sub>9</sub>, F<sub>9</sub>
10. x<sub>10</sub>, F<sub>10</sub>

Recycle ratio, *r*

# References

1. EIA *International Energy Outlook 2009*; DOE/EIA-0484(2009); U.S. Energy Information Administration (EIA): 2009.
2. Hegerl, G. C.; Zwiers, F. W.; Braconnot, P.; Gillett, N. P.; Luo, Y.; Marengo Orsini, J. A.; Nicholls, N.; Penner, J. E.; Stott, P. A., IPCC 2007: Understanding and Attributing Climate Change, Working Group 1 in the 4th Assessment Report of the Intergovernmental Panel on Climate Change. *Report 2007*, 84.
3. Haynes, B. S.; Neville, M. N.; Quann, R. J.; Sarofim, A. F., Factors governing the surface enrichment of fly ash in volatile trace species. *Journal of Colloid and Interface Science* **1982**, 87, (1), 266-278.
4. Suriyawong, A.; Hogan, C. J.; Jiang, J.; Biswas, P., Charged fraction and electrostatic collection of ultrafine and submicrometer particles formed during O<sub>2</sub>-CO<sub>2</sub> coal combustion. *Fuel* **2008**, 87, (6), 673-682.
5. Li, Y.; Suriyawong, A.; Daukoru, M.; Zhuang, Y.; Biswas, P., Measurement and Capture of Fine and Ultrafine Particles from a Pilot-Scale Pulverized Coal Combustor with an Electrostatic Precipitator. *J. Air & Waste Manage. Assoc.* **2009**, 59, (5), 553-9.
6. Zhuang, Y.; Biswas, P., Submicrometer Particle Formation and Control in a Bench-Scale Pulverized Coal Combustor. *Energy & Fuels* **2001**, 15, (3), 510-516.
7. Huang, S.-H.; Chen, C.-C., Ultrafine Aerosol Penetration through Electrostatic Precipitators. *Environ. Sci. Technol.* **2002**, 36, (21), 4625-4632.
8. Ylätaalo, S. I.; Hautanen, J., Electrostatic Precipitator Penetration Function for Pulverized Coal Combustion. *Aerosol Sc. & Tech.* **1998**, 29, (1), 17-30.
9. Linak, W. P.; Yoo, J.-I.; Wasson, S. J.; Zhu, W.; Wendt, J. O. L.; Huggins, F. E.; Chen, Y.; Shah, N.; Huffman, G. P.; Gilmour, M. I., Ultrafine ash aerosols from coal combustion: Characterization and health effects. *P Combust Inst* **2007**, 31, 1929-1937.

10. Samet, J. M.; Dominici, F.; Curriero, F. C.; Coursac, I.; Zeger, S. L., Fine particulate air pollution and mortality in 20 US cities, 1987-1994. *New England journal of medicine* **2000**, 343, (24), 1742.
11. Ramanathan, V.; Crutzen, P. J.; Kiehl, J. T.; Rosenfeld, D., Aerosols, Climate, and the Hydrological Cycle. *Science* **2001**, 294, (5549), 2119-2124.
12. Dockery, D. W.; Pope, C. A.; Xu, X.; Spengler, J. D.; Ware, J. H.; Fay, M. E.; Ferris, B. G.; Speizer, F. E., An association between air pollution and mortality in six US cities. *The New England journal of medicine* **1993**, 329, (24), 1753.
13. Pope III, C. A.; Thun, M. J.; Namboodiri, M. M.; Dockery, D. W.; Evans, J. S.; Speizer, F. E.; Heath Jr, C. W., Particulate air pollution as a predictor of mortality in a prospective study of US adults. *American journal of respiratory and critical care medicine* **1995**, 151, (3), 669.
14. Epstein, N., *Particulate fouling of heat transfer surfaces: mechanisms and models*. NATO Advanced Study Institute Series E, Kluwer Academic Publishers: Dordrecht; Boston, 1988; Vol. 145.
15. *CO2 Emissions from Fuel Combustion Highlights*; International Energy Agency: 2009.
16. Baumert, K. A.; Herzog, T.; Pershing, J. *Navigating the Numbers: Greenhouse Gas Data and International Climate Policy*; World Resources Institute: 2005; p 61.
17. *Emissions of Greenhouse Gases Report*; DOE/EIA-0573(2007); Energy Information Administration: 2008.
18. Abraham, B. M.; Asbury, J. G.; Lynch, E. P.; Teotia, A. P. S., Coal-oxygen process provides carbon dioxide for enhanced recovery. *Oil Gas J* **1982**, 80, (11), 68-70.
19. Buhre, B.; Elliott, L.; Sheng, C.; Gupta, R. P.; Wall, T. F., Oxy-fuel combustion technology for coal-fired power generation. *Progress in Energy and Combustion Science* **2005**, 31, (4), 283-307.
20. Croiset, E.; Thambimuthu, K., Coal combustion with flue gas recirculation for CO<sub>2</sub> recovery. In *Greenhouse gas technologies*, Riemer, P.; Eliasson, B.; Wokaun, A., Eds. Elsevier Science: Amsterdam, 1999; pp 581-6.
21. Okazaki, K.; Ando, T., NO<sub>x</sub> reduction mechanism in coal combustion with recycled CO<sub>2</sub>. *Energy* **1997**, 22, (2/3).

22. Hu, Y. Q.; Kobayashi, N.; Hasatani, M., The reduction of recycled-NO<sub>x</sub> in coal combustion with O<sub>2</sub>/recycled flue gas under low recycling ratio. *Fuel* **2001**, 80, (13), 1851-1855.
23. Hu, Y. Q.; Kobayashi, N.; Hasatani, M., Effects of coal properties on recycled-NO<sub>x</sub> reduction in coal combustion with O<sub>2</sub>/recycled flue gas. *Energy Conversion and Management* **2003**, 44, (14), 2331-2340.
24. Seepana, S.; Jayanti, S., Optimized enriched CO<sub>2</sub> recycle oxy-fuel combustion for high ash coals. *Fuel* **2009**, 1-9.
25. Tan, Y.; Croiset, E.; Douglas, M. A.; Thambimuthu, K. V., Combustion characteristics of coal in a mixture of oxygen and recycled flue gas. *Fuel* **2006**, 85, (4), 507-512.
26. Singh, D.; Croiset, P.; Douglas, P. L.; Douglas, M. A., Techno-economic study of CO<sub>2</sub> capture from an existing coal-fired power plant: MEA scrubbing Vs. O<sub>2</sub>/CO<sub>2</sub> recycle combustion. *Energy Convers Manage* **2003**, 44, 3073-3091.
27. Beér, J. M., High efficiency electric power generation: The environmental role. *Progress in Energy and Combustion Science* **2007**, 33, (2), 107-134.
28. Vattenfall's project on CCS - Schwarze Pumpe. [http://www.vattenfall.com/www/co2\\_en/co2\\_en/879177tbd/879211pilot/901887test/index.jsp](http://www.vattenfall.com/www/co2_en/co2_en/879177tbd/879211pilot/901887test/index.jsp) (October 27, 2009),
29. Mcdonald, D. K.; Flynn, T. J.; DeVault, D. J.; Varagani, R.; Levesque, S.; Castor, W., 30 MWt Clean Environment Development Oxy-Coal Combustion Test Program. In *33rd International Technical Conference on Coal Utilization & Fuel Systems*, Clearwater, FL, 2008.
30. Suriyawong, A.; Gamble, M.; Lee, M.-H.; Axelbaum, R.; Biswas, P., Submicrometer Particle Formation and Mercury Speciation Under O<sub>2</sub>-CO<sub>2</sub> Coal Combustion. *Energy & Fuels* **2006**, 20, 2357-2363.
31. Sheng, C.; Li, Y., Experimental study of ash formation during pulverized coal combustion in O<sub>2</sub>/CO<sub>2</sub> mixtures. *Fuel* **2008**, 87, (7), 1297-1305.
32. Sheng, C.; Lu, Y.; Gao, X.; Yao, H., Fine Ash Formation during Pulverized Coal Combustion--A Comparison of O<sub>2</sub>/CO<sub>2</sub> Combustion versus Air Combustion. *Energy & Fuels* **2007**, 21, 435-440.

33. Quann, R. J. Ash Vaporization Under Simulated Pulverized Coal Combustion Conditions (Ph.D. Thesis). Massachusetts Institute of Technology, Cambridge, MA, 1982.
34. Quann, R. J.; Neville, M.; Sarofim, A. F., A Laboratory Study of the Effect of Coal Selection on the Amount and Composition of Combustion Generated Submicron Particles. *Combustion Sc. & Tech.* **1990**, 74, (1), 245-265.
35. Smith, K. L., *The structure and reaction processes of coal*. Plenum Press: New York, NY, 1994.
36. Vassilev, S. V.; Kitano, K.; Vassileva, C. G., Some relationships between coal rank and chemical and mineral composition. *Fuel* **1996**, 75, (13), 1537-1542.
37. Linak, W. P., Toxic Metal Emissions from Incineration: Mechanisms and Control. *Progress in Energy and Combustion Science* **1993**, 19, (2), 145-185.
38. Linak, W. P.; Wendt, J. O. L., Trace metal transformation mechanisms during coal combustion. *Fuel Processing Technology* **1994**, 39, 173-198.
39. Scotto, M. V.; Uberoi, M.; Peterson, T. W.; Shadman, F.; Wendt, J. O. L., Metal capture by sorbents in combustion processes. *Fuel Processing Technology* **1994**, 39, (1-3), 357-372.
40. Biswas, P.; Wu, C. Y., Control of Toxic Metal Emissions from Combustors Using Sorbents: A Review. *Journal of the Air & Waste Management Association* **1998**, 48, (3), 113-127.
41. Yan, R.; Gauthier, D.; Flamant, G., Partitioning of Trace Elements in the Flue Gas from Coal Combustion. *Combustion and Flame* **2001**, 125, 942-954.
42. Mulholland, J. A.; Sarofim, A. F., Mechanisms of inorganic particle formation during suspension heating of simulated aqueous wastes. *Environmental Science & Technology* **1991**, 25, (2), 268-274.
43. Senior, C. L.; Flagan, R. C., Ash Vaporization and Condensation During Combustion of a Suspended Coal Particle. *Aerosol Sc. & Tech.* **1982**, 1, (4), 371-383.
44. Quann, R. J.; Neville, M.; Janghorbani, M.; Mims, C. A.; Sarofim, A. F., Mineral Matter and Trace-Element Vaporization in a Laboratory-Pulverized Coal Combustion System. *Environ. Sci. Technol.* **1982**, 16, 776-781.

45. Damle, A. S.; Ensor, D. S.; Ranade, M. B., Coal Combustion Aerosol Formation Mechanisms: A Review. *Aerosol Sc. & Tech.* **1982**, 1, (1), 119-133.
46. Zhuang, Y. Experimental and theoretical study of submicrometer particle formation and capture mechanisms in coal combustion environments (Ph.D. Thesis). University of Cincinnati, Cincinnati, OH, 2000.
47. Flagan, R. C., Submicron particles from coal combustion. *Symposium (International) on Combustion* **1979**, 17, (1), 97-104.
48. Senior, C. L.; Panagiotou, T.; Sarofim, A. F.; Helble, J. J., Formation of Ultrafine Particulate Matter from Pulverized Coal Combustion. In *219th American Chemical Society National Conference*, American Chemical Society: San Francisco, CA, 2000; Vol. 45.
49. Fletcher, T. H.; Ma, J.; Rigby, J. R.; Brown, A. L.; Webb, B. W., Soot in Coal Combustion Systems. *Progress in Energy and Combustion Science* **1997**, 23, 283-301.
50. Veranth, J. M.; Fletcher, T. H.; Pershing, D. W.; Sarofim, A. F., Measurement of soot and char in pulverized coal fly ash. *Fuel* **2000**, 79, (9), 1067-1075.
51. Smallwood, M. Mercury Capture in Coal Combustors (M.S. Thesis). Washington University in St. Louis, St. Louis, MO, 2005.
52. Suriyawong, A. Oxy-Coal Combustion: Fine Particle & Mercury Emissions and Control (Ph.D. Thesis). Washington University in St. Louis, St. Louis, MO, 2009.
53. Reynolds, W. C. *The Element Potential Method for Chemical Equilibrium Analysis: Implementation in the Interactive Program STANJAN*; Dept. of Mechanical Engineering, Stanford University: Stanford, CA, 1986.
54. Kiga, T., O<sub>2</sub>/RFG combustion-applied pulverised coal fired plant for CO<sub>2</sub> recovery. In *Advanced Coal Combustion*, Miura, T., Ed. Nova Science Publishers, Huntington, NY: 2001.
55. Liu, H.; Zailani, R.; Gibbs, B., Comparisons of pulverized coal combustion in air and in mixtures of O<sub>2</sub>/CO<sub>2</sub>. *Fuel* **2005**, 84, (7-8), 833-840.
56. Murphy, J. J.; Shaddix, C. R., Combustion kinetics of coal chars in oxygen-enriched environments. *Combustion and Flame* **2006**, 144, (4), 710-729.

57. Shaddix, C., Coal Particle Ignition, Devolatilisation & Char Combustion Kinetics During Oxy-Combustion. In *Intl. Oxy-Combustion Research Network*, IEA Greenhouse Gas R&D Programme: Windsor, CT, 2007.
58. Linak, W. P.; Peterson, T. W., Effect of Coal Type and Residence Time on the Submicron Aerosol Distribution from Pulverized Coal Combustion. *Aerosol Sc. & Tech.* **1984**, 3, (1), 77-96.
59. Nozaki, T.; Takano, S.; Kiga, T.; Omata, K.; Kimura, N., Analysis of the Flame Formed During Oxidation of Pulverized Coal by an O<sub>2</sub>-CO<sub>2</sub> Mixture. *Energy* **1997**, 22, (2/3), 199-205.
60. Bejarano, P. A.; Levendis, Y. A., Single-coal-particle combustion in O<sub>2</sub>-N<sub>2</sub> and O<sub>2</sub>/CO<sub>2</sub> environments. *Combustion and Flame* **2008**, 153, (1-2), 270-287.
61. Buhre, B. J. P.; Hinkley, J. T.; Gupta, R. P.; Nelson, P. F.; Wall, T. F., Fine ash formation during combustion of pulverised coal--coal property impacts. *Fuel* **2006**, 85, 185-193.
62. EIA *Annual Coal Report 2008*; DOE/EIA-0584 (2008); U.S. Energy Information Administration (EIA): 2008.
63. Wibberley, L. J. Alkali Ash Reactions and Deposit Formation in Pulverized Coal Boilers (Ph.D. Thesis). University of Newcastle, New South Wales, Australia, 1980.
64. Zhang, L.; Binner, E.; Qiao, Y.; Li, C.-Z., High-Speed Camera Observation of Coal Combustion in Air and O<sub>2</sub>/CO<sub>2</sub> Mixtures and Measurement of Burning Coal Particle Velocity. *Energy & Fuels* **2010**, 24, (1), 29-37.

# Vita

## S. Michael Daukoru

<b>Date of Birth</b>	October 23, 1984
<b>Place of Birth</b>	Warri, Nigeria
<b>Degrees</b>	Texas Tech University, Lubbock, TX B.S. Summa Cum Laude, Mechanical Engineering, Dec. 2004  Stanford University, Stanford, CA M.S. Mechanical Engineering, Jan. 2007
<b>Professional Societies</b>	American Society of Mechanical Engineers (ASME)
<b>Publications</b>	Li, Y., <b>Daukoru, M.</b> , Suriyawong, A., Biswas, P. (2009) Mercury Emissions Control in Coal Combustion Systems Using Potassium Iodide: Bench- and Pilot-Scale Studies, <i>Energy &amp; Fuels</i> . 23(1): 236–243.  Li, Y., Suriyawong, A., <b>Daukoru, M.</b> , Zhuang, Y., Biswas, P. (2009) Measurement and Capture of Fine and Ultrafine Particles from a Pilot-Scale Pulverized Coal Combustor with an Electrostatic Precipitator, <i>J. Air and Waste Management Assoc.</i> 59(5): 553-9.
<b>Courses Completed</b>	Transport Phenomena A Mathematical Methods in Chemical Engineering B Aerosol Science & Technology A Kinetics and Reaction Engineering Principles B Advanced Topics in Aerosol Science & Engineering B- Radiation Heat Transfer A+ Special Topics in Phys. Chem.: Surface Chemistry B Measurement Techniques for Particle Characterization B+

August 2010

**Oxy-Combustion of US & China Coals,**

**Daukoru, M.S. 2010**